Low water levels in Panama Canal due to increasing demand exacerbated by El Niño event

Authors

Clair Barnes, *Grantham Institute, Imperial College London, UK*
Steve Paton, *Smithsonian Tropical Research Institute, Panama*
Robert F Stallard, *Smithsonian Tropical Research Institute, Panama & Institute of Arctic and Alpine Research, University of Colorado, Boulder, US*
Hector de Lima, *Autoridad del Canal Panama, Panama*
Ben Clarke, *Grantham Institute, Imperial College London, UK*
Maja Vahlberg, *Red Cross Red Crescent Climate Centre, the Hague, Netherlands (based in Ubmeje/Umeå, Sweden)*
Adwoa Amakona, *Red Cross Red Crescent Climate Centre, the Hague, Netherlands (based in London, UK)*
Karina Izquierdo, *Red Cross Red Crescent Climate Centre, the Hague, Netherlands (based in London, UK)*
Sajanika Sivanu, *Red Cross Red Crescent Climate Centre, the Hague, Netherlands (based in Bonn, Germany)*
Fredi Otto, *Grantham Institute, Imperial College London, UK*

Review authors

Mariam Zachariah, *Grantham Institute, Imperial College London, UK*
Sjoukje Philip, *Royal Netherlands Meteorological Institute (KNMI), De Bilt, The Netherlands*
Malcolm Mistry, *Red Cross Red Crescent Climate Centre, the Hague, Netherlands (based in London, UK)*
Roop Singh, *Red Cross Red Crescent Climate Centre, the Hague, Netherlands (based in New Jersey, USA)*
Julie Arrighi, *Red Cross Red Crescent Climate Centre, the Hague, Netherlands; Global Disaster Preparedness Center, Washington DC, USA; University of Twente, Enschede, The Netherlands (based in New York, USA)*

1 Introduction

Since early 2023, the Republic of Panama has experienced one of the driest years on record. Precipitation from the area of the Panama Canal Watershed (PCW), source of 100% of the water used by the Panama Canal for its operations, was below average for all but one of the 8 months that make up Panama's rainy season. Beginning in June of that year, the Panama Canal Authority found it necessary to begin to restrict both the number and size of ships passing through the Panama Canal due to much below average rainfall and historically low (for the time of year) water levels in Gatún Lake - principal hydrological reserve for the Canal - immediately causing disruptions to global shipping that continue into early 2024 (Figure 1.1).

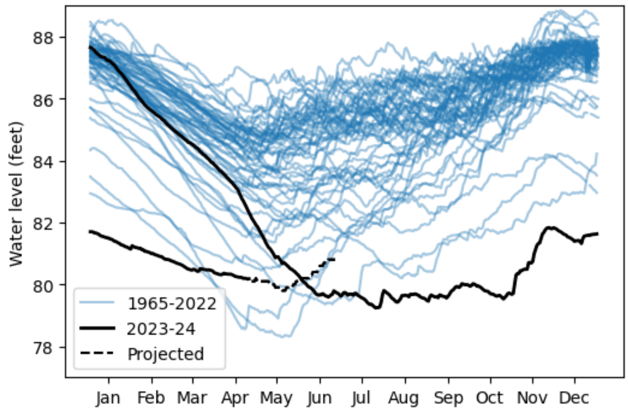

Figure 1.1: *Historic levels of Gatún Lake (1965-2024) with 2023-2024 highlighted; based on [data from the Panama Canal Authority](#) (ACP)*

Between 1997 and 2023, the PCW has experienced three of the driest years ever recorded (data first collected in 1880): 1997, 2015 and 2023, as well as the three driest years in a row, 2013-15 (STRI, ACP). During this same period, the watershed has experienced 8 of its 10 greatest storms, including the single largest storm in 2010 called 'La Purisima'. The operations of the Panama Canal, as well as access to fresh water for approximately 55% of Panama's population, are directly affected by these extreme rainfall events.

Approximately 55% (1,598 km^2) of the PCW is under forest (old and new growth lowland tropical rainforest with areas of commercial reforestation, mostly teak). Two-thirds of the forested watershed lies in protected areas, much of which was established beginning in 1980. Vegetation in the remaining areas comprises grassland (29%), shrubland (10%), commercial tree plantations (2%), and urban areas (3%). Agriculture accounts for less than 1% of the watershed area (Simonit and Perrings, 2013).

Rainfall in the PCW, as well as over most of Panama, is divided into two distinct seasons, a dry season that begins around the end of December and extends to the beginning of May, and the 8-month wet season (Figure 1.2a). Compared to the wet season, the dry season is a period of significantly higher solar radiation, stronger winds, lower relative humidity, and much higher evapotranspiration. On average, approximately 10-11% of the yearly rainfall and 48% of the evapotranspiration occurs during the 4-month dry season (based on STRI/ACP station data for Barro Colorado Island and precipitation at all stations).

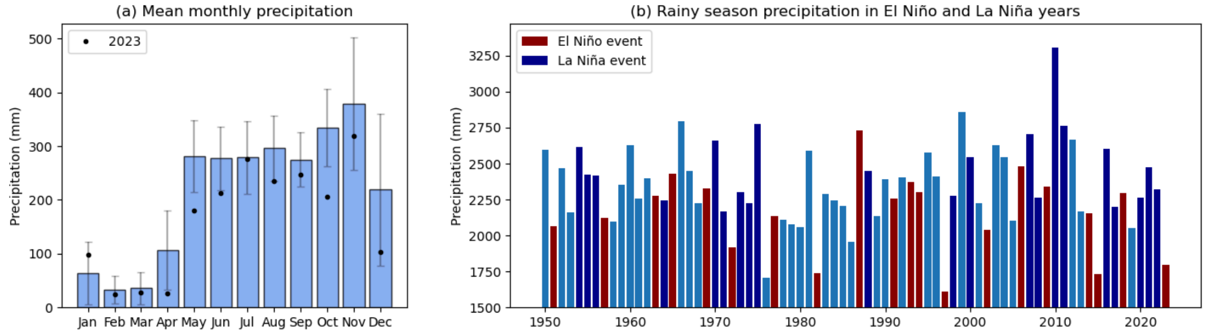

Figure 1.2: *(a) Monthly mean precipitation over the available stations (1881-2023). Vertical lines indicate 1 standard deviation above/below the mean. Black points indicate the 2023 precipitation. (b) Total rainy season precipitation over the available stations (axes truncated) with Niño years coloured red and Niña years coloured blue. Niño/Niña classifications obtained from the Australian Bureau of Meteorology prior to 2016 and NCEP thereafter.*

One of the primary drivers for years of below average rainfall in Panama, as well as much of Central America and the Caribbean is the warm 'El Niño' phase of the El Niño Southern Oscillation (ENSO) phenomenon. Since 1950, 5 of the 7 driest years for the PCW have occurred during major El Niño events. During the same period, 4 of the 8 wettest years occurred during major La Niña years (Figure 1.2b). As a result of El Niño-related below average rainfall, the Panama Canal Authority was forced to significantly reduce both the number of ships and their maximum size in 1998, 2016 and 2023/4. The city of Panama was forced to implement severe water rationing 1998 and 2016. At the time of writing, at the end of April 2024, forecasts are for above average rainfall at the beginning of May, and water rationing is therefore not expected to be necessary as a result of the low rainfall during 2023.

Analysis of observational data suggests that, up to 2014, there was no statistically significant drying trend in Panama, in contrast to most of Central America (CA) which shows local drying trends in the 12-month standardised precipitation index (Muñoz-Jiménez et al., 2019). Further north, in a region stretching from southern Mexico down to Costa Rica (just north of Panama), a significant trend in decreased summertime rainfall has been observed since 1979 (Pascale et al., 2021). While this trend was not attributed to anthropogenic climate change (ACC), the 5-year drought in the same region in the summer months of 2015-2019 (inclusive) was found to have become around four times more likely due to ACC (Pascale et al., 2021).

The climate of CA is characterised as monsoonal, with two distinct peaks divided by a 'mid-summer drought' in July-August (Imbach et al., 2018). However, as seen in Figure 1.2a, in Panama rainfall across the wet season is much more consistent, with no mid-summer drought period. It is therefore challenging to extrapolate results intra-regionally and may explain the apparent disagreement in observed trends within the region. Indeed, working group 1 of AR6 of the IPCC found that in southern Central America there had been mixed trends across different drought metrics and subregions (Seneviratne et al., 2021).

Panama is a comparatively small nation, dividing the Atlantic and Pacific oceans by only around 80 km at its narrowest, and has extremely complex topography (Imbach et al., 2018). This makes projections challenging with global climate models, which typically have horizontal resolutions of at least 100km. Nonetheless, projections of drought on the global scale show decreasing drought in Panama in contrast to most of Central and South America, and southern North America (Dai, 2013).

This further adds to the intra-regional complexity of changes in rainfall and drought. However, recent studies using high-resolution climate models, either regional or high-resolution general circulation models, are increasingly able to capture the appropriate scales (~tens of km). Using CORDEX Central America with models at approximately 25 km, it was found that the wider CA region has several 'dry hotspots' that became drier from 1980-2010 due to both rainfall deficits and temperature increases (Gomez and Cavazos, 2024). However, in Panama differences between different observation and model datasets, and consistently weak signals, mean that no significant changes can be identified (Gomez and Cavazos, 2024).

Another study using the 'Eta Regional Climate Model' at 8 km resolution and projected using the RCP4.5 scenario showed that precipitation during the rainy season is expected to decrease generally in the CA region. Furthermore, it showed that water availability in Panama is likely to decrease (except for the western coast), that a mid-summer drought may develop, and that there is no notable change in the number of consecutive dry days (Imbach et al., 2018). Meanwhile, a study using 20 km and 60 km atmospheric general circulation models projected an increase in December-February rainfall in eastern Panama and a decrease in June-August rainfall in the west (Nakaegawa & Mizuta, 2023). The latter is entirely within the rainy season so is more important for overall water availability. Finally, an earlier study using the same models explicitly calculated the change in consecutive dry days, finding an expected increase over much of Panama (Kusunoki et al., 2019).

Other characteristics of the CA climate are also changing. For instance, the changes in drought rates are also coupled with projected increases in extreme precipitation days in Panama, which may also lead to severe impacts on the region (Nakaegawa & Mizuta, 2023; Imbach et al., 2018). Studies also project a significant warming trend across CA including Panama (Imbach et al., 2018). This is known to contribute to drought in other tropical regions, including the Amazon and tropical Africa, through increased evaporation from the land surface (WWA, 2024; Spinoni et al., 2020). Given this complex picture and the importance of rainfall and water availability in Panama for local people and the global economy alike, an attribution study focusing directly on this region may help to elucidate the potentially crucial role of ACC.

1.1 Event definition

In this study we focus on the low precipitation observed across the Gatún Lake catchment during the 2023 rainy season (May-December). The study region, shown in Figure 1.3, encompasses the lake catchment (outlined in red) and surrounding area. We primarily analyse the time series of accumulated precipitation during the rainy season over all land cells in this region. A secondary analysis investigates changes in potential evapotranspiration during both the dry and rainy seasons in the same region. Lake levels did not begin to drop below seasonally normal levels until May 2023 (Figure 1.1), and almost all of the 2023 precipitation deficit occurred during the rainy season, so we do not analyse changes in precipitation during the January-April dry season here.

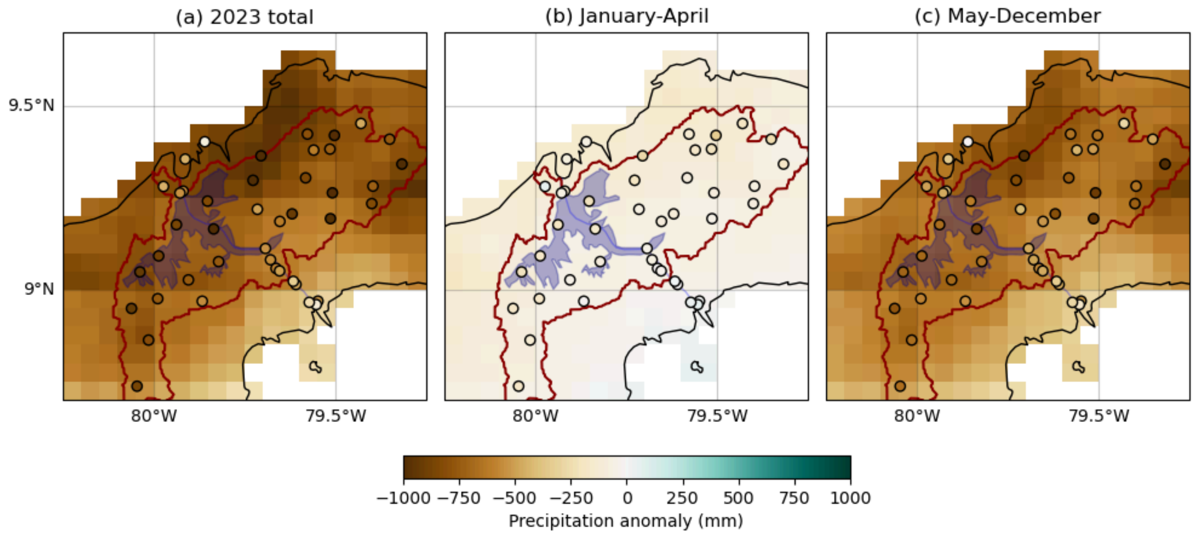

Figure 1.3: *Maps of the 2023 precipitation deficit with respect to the 1990-2020 climatology in the CHIRPS dataset and 43 ACP stations, during (a) the whole year; (b) the January-April dry season; (c) the May-December rainy season. Gatún Lake is shaded blue, and the catchment is outlined in dark red.*

2 Data and methods

2.1 Observational data

2.1.1 Composite of station data

The Panama Canal Authority (ACP) and the Smithsonian Tropical Research Institute (STRI) operate a combined network of approximately 65 meteorological stations in and around the watershed. This network provides one of the best rainfall records (both in terms of duration and data quality) for Central America and the Caribbean. These data - which are freely available from both the ACP and STRI websites - permit the exploration of both the spatial and temporal variability in PCW rainfall patterns not possible almost anywhere else in the region. The longest stations date back to 1881 although the majority became operational much later. The mean of the station data from 1925-2023, with missing values imputed using multiple linear regression over sites with similar but more complete precipitation series, is used in the analysis in Section 3.2 as a proxy for the mean precipitation over the study region. This start date was chosen to take advantage of the longer time series without relying too heavily on the imputed data; however, the results of the analysis were not found to be sensitive to the length of the time series used, or to whether all stations or only a subset of mostly-complete stations were included in the composite (Section 3.2.1). The reconstructed time series data are currently in preparation for publication.

2.1.2 Gridded data products

Gridded precipitation data were obtained from CHIRPS, ERA5-Land and MSWEP. Potential evapotranspiration was taken from ERA5-Land and TerraClimate.

1. CHIRPS (Climate Hazards Group InfraRed Precipitation with Station data; Funk et al., 2015b), a daily dataset developed by the UC Santa Barbara Climate Hazards Group, incorporating satellite data, infrared Cold Cloud Duration (CCD) estimates and blended station data. Daily data are available from 1981-present at 0.05° resolution from 60S to 60N.

2. ERA5-Land (Muñoz-Sabater et al., 2021) produced by the European Centre for Medium-Range Weather Forecasts. This product is a replay of the land component of the ERA5 climate reanalysis with a finer spatial resolution of 0.1° (~9km grid spacing), at hourly time steps from 1950 to 5 days before the current date. The land model used is the tiled ECMWF Scheme for Surface Exchanges over Land incorporating land surface hydrology (H-TESSEL).

3. MSWEP (Multi-Source Weighted-Ensemble Precipitation) v2.8 dataset (updated from Beck et al., 2019), which combines gauge, satellite, and reanalysis-based data. Data is available at 3-hourly intervals from 1979 to ~3 hours from real-time, and at 0.1° spatial resolution globally.

4. TerraClimate (Abatzoglou et al., 2018), a dataset of monthly climate and climatic water balance for global terrestrial surfaces from 1958-2023 at ~4-km (1/24th degree) spatial resolution. TerraClimate uses climatically aided interpolation, combining high-spatial resolution climatological normals from the WorldClim dataset, with coarser spatial resolution, but time-varying data from CRU Ts4.0 and, where no climate stations are available in CRU, the Japanese 55-year Reanalysis (JRA55).

2.1.2 Large-scale climate indices

As a proxy for anthropogenic climate change we use the (low-pass filtered) global mean surface temperature (GMST) taken from the National Aeronautics and Space Administration (NASA) Goddard Institute for Space Science (GISS) surface temperature analysis (GISTEMP, Hansen et al., 2010 and Lenssen et al., 2019).

The detrended Niño3.4 index is computed from NOAA's ERSST v.5 sea surface temperatures, by subtracting the mean tropical SST (20S-20N) from the mean SST over the Nino3.4 region (5S-5N, 170W-120W) (van Oldenborgh et al., 2021).

2.2 Climate model and experiment descriptions

1. High-resolution regional climate model data were obtained from the Coordinated Regional Climate Downscaling Experiment (CORDEX) multi-model ensemble (Gutowski et al., 2016; Giorgi et al., 2021). For the Central America domain, the ensemble consists of 9 simulations resulting from pairings of 6 Global Climate Models (GCMs) and 3 Regional Climate Models (RCMs) at 0.22° resolution (CAM-22), and 10 simulations resulting from pairings of 9 GCMs and 2 RCMs at 0.44° resolution (CAM-44). For the South America domain, the ensemble consists of 6 simulations resulting from pairings of 3 GCMs and 2 RCMs at 0.22° resolution (SAM-22) and 10 simulations resulting from 10 pairings of 9 GCMs and 2 RCMs at 0.44°

resolution (SAM-44). These simulations are driven by historical forcings up to 2005, and extended to the year 2100 using the RCP8.5 scenario.

2.3 Statistical methods

Methods for observational and model analysis and for model evaluation and synthesis are used according to the World Weather Attribution Protocol, described in Philip et al. (2020), with supporting details found in van Oldenborgh et al. (2021), Ciavarella et al. (2021) and here. The key steps, presented in sections 3-6, are: (3) trend estimation from observations; (4) model validation; (5) multi-method multi-model attribution; and (6) synthesis of the attribution statement.

In this report we analyse annual time series of accumulated precipitation and accumulated PET over the Gatún Lake catchment shown in Figure 1.1.

A nonstationary normal distribution is used to model both of these variables. For precipitation, the distribution is assumed to scale exponentially with the covariates, with the dispersion (the ratio between the standard deviation and the mean) remaining constant over time; while for PET, the distribution is assumed to shift linearly with the covariates, while the variance remains constant. The parameters of the statistical model are estimated using maximum likelihood.

For each time series we calculate the return periods, probability ratio (PR; the factor-change in the event's probability) and change in intensity of the event under study for the 2023 GMST and for 1.2°C cooler GMST: this allows us to compare the climate of now and of the preindustrial past (1850-1900, based on the Global Warming Index).

2.3.1 Statistical modelling of the combined effect of GMST and ENSO

As noted in Section 1, precipitation in Panama is known to be influenced by natural modes of variability, particularly the ENSO, with positive ENSO phases (El Niño events) associated with late onset and early finish of the rainy season, as well as lower rainfall intensity during the rainy months.

In order to examine the effect of the ENSO on rainy-season precipitation alongside that of increasing GMST, we extend the nonstationary model to accommodate an additional covariate. The variable of interest, X, is assumed to follow a normal distribution in which the location and scale parameters vary with both GMST and ENSO:

$$X \sim N(\mu, \sigma \mid \mu_0, \sigma_0, \alpha, \beta, T, I),$$

where X denotes the variable of interest, rainy-season precipitation; T is the smoothed GMST, I is the detrended Niño3.4 index, μ_0 and σ_0 are the mean and variance parameters of the nonstationary distribution and α, β are the trends due to GMST and ENSO, respectively. As a result, the location and scale of the distribution have a different value in each year, determined by both the GMST and Niño3.4 states. Maximum likelihood estimation is used to estimate the model parameters, with

$$\mu = \mu_0 exp\left(\frac{\alpha T + \beta I}{\mu_o}\right) \quad \text{and} \quad \sigma = \sigma_0 exp\left(\frac{\alpha T + \beta I}{\mu_o}\right).$$

This formulation reflects the Clausius Clapeyron relation, which implies that precipitation scales exponentially with temperature (Trenberth et.al., 2003, O'Gorman and Schneider 2009), and so that precipitation will scale exponentially with the strength of the detrended Niño3.4 index. Under this model, the effects of GMST and the detrended Niño3.4 index are assumed to be independent of one another, so that the change in intensity due to GMST is unaffected by the change in intensity due to the ENSO phase. We note that this may not be the case in the real world, as the intensity and frequency of El Niño events may have been influenced by climate change (Cai et al., 2021); however, by using a detrended Niño3.4 index (see Section 2.1.2) we aim to minimise the correlation between the two factors, and so do not expect the qualitative findings of this study to be affected by this simplifying assumption.

2.3.2 Estimation of return periods

Extra care must be taken when reporting and interpreting return periods that depend on more than one covariate. Typically, WWA reports estimated return periods for the event of interest under current climatic conditions: in this case, with the GMST fixed at the 2023 level. In this study, there are two covariates to consider: the GMST and detrended Niño3.4 index. By fixing both Niño3.4 and the GMST at their 2023 levels, we can estimate the return period of the 2023 event in the current climate and in the current ENSO state. Mathematically, this return period is written as

$$1 / P(X > x_{2023} \,|\, T = t_{2023}, I = i_{2023}),$$

where x_{2023} is the 2023 value of observed precipitation; t_{2023} denotes the 2023 GMST; and i_{2023} denotes the mean of the detrended Niño3.4 index from May-December 2023. Altogether, the expression in brackets gives the probability that X will exceed x_{2023}, given that $T = t_{2023}$ and $I = i_{2023}$; inverting this probability gives us an expected return period, in years.

However, this return period only tells us the probability of experiencing a similar event under current Niño3.4 conditions and current warming levels. In order to understand how frequently such an event is actually likely to occur, we must account for the fact that the Niño3.4 is not often in the positive phase observed in 2023. To do this, we evaluate the return period over all states of the Niño3.4 that have been recorded since 1980 (the period covered by the available gridded data products). This is done by first averaging the probability of exceeding x_{2023} over all recorded values of i_{2023} during this period, then inverting to obtain the return period:

$$1 / \sum_{y=1980}^{2023} P(X > x_{2023} \,|\, T = t_{2023}, I = i_y).$$

2.3.3 Defining the ENSO state in climate models

The multi-method multi-model attribution step of the WWA protocol involves estimating, for each climate model, the effective return level of a 1-in-*n*-year event under the current climate state, and estimating the expected change in likelihood and intensity of such an event after a specified change in the covariates. Because the smoothed GMST is generally monotonically increasing, the standard WWA approach is simply to take the model's 2023 GMST as a covariate and to estimate the expected magnitude of an *n*-year event. However, the factual climate in this study is defined by the 2023 GMST and by the mean of the detrended Niño3.4 index during the rainy season. During the attribution step, the detrended Niño3.4 index derived from the climate model is standardised so that the subset from 1979-2023 has mean 0 and variance 1; the 'factual' climate is then defined as having the model's 2023 GMST and the 2023 observed value of the detrended Niño3.4 index, standardised in the same way. This removes any potential biases in the results due to differences between the amplitude of the modelled Niño3.4 index and that observed.

3 Observational analysis: return period and trend

3.1 Evaluation of gridded precipitation products

Figure 3.1 shows the observed precipitation during the 2023 rainy season in three gridded data products, along with the values recorded at 57 ACP stations where data for the entire season was available. In the station data the stations further to the north of the region tend to be wetter, while those toward the Pacific Coast received less precipitation. CHIRPS captures this pattern rather well; MSWP is generally too wet over Gatún Lake and further south; and ERA5-Land records extremely low precipitation for the 2023 rainy season. As a result, CHIRPS records 15-30% less precipitation across the region than the 1990-2020 mean (Figure 3.2); MSWEP records above-average precipitation in some regions, with a deficit in others of up to 25%; and ERA5-Land has around 60% less precipitation than a typical season. The stations record up to 40% less precipitation than in a typical rainy season from 1990-2020. This corresponds to a mean deficit across the region of 685mm in CHIRPS; 210mm in MSWEP; nearly 2000mm in ERA5-Land; and 706mm in the ACP stations.

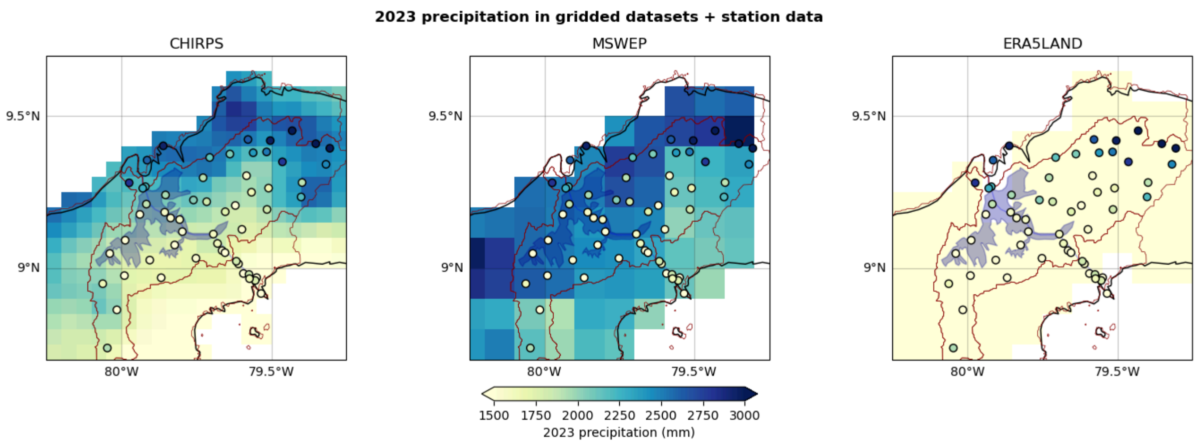

Figure 3.1: *Maps of accumulated precipitation over the 2023 rainy season (May-December). Circles represent observed precipitation at 57 stations monitored by the ACP. Gatún Lake is shaded blue.*

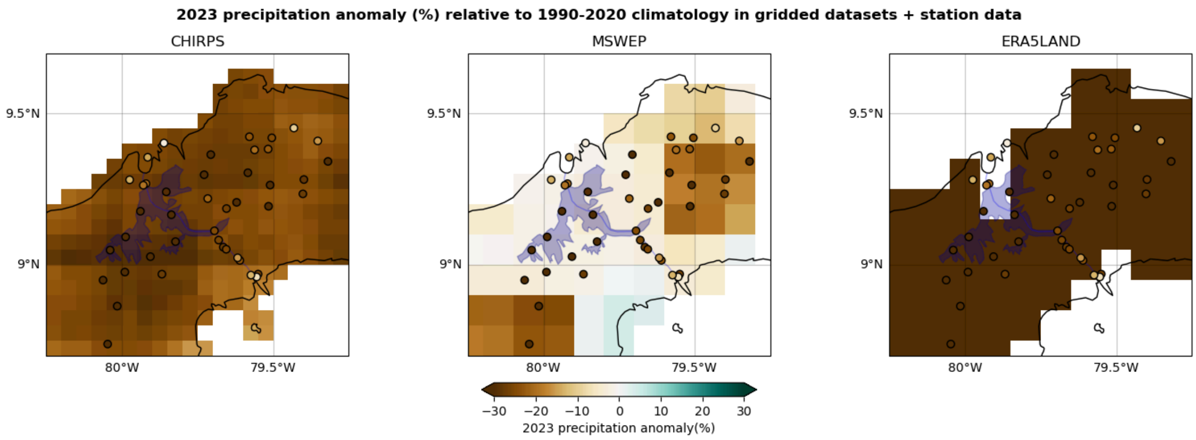

Figure 3.2: *Maps of relative accumulated precipitation anomalies over the 2023 rainy season (May-December) with respect to the 1990-2023 climatology. Circles represent observed precipitation at 43 stations monitored by the ACP for which data was available during the reference period.*

Figure 3.3 shows maps of the estimated relative change in May-December precipitation associated with a 1.2°C increase in GMST, estimated using a statistical model in which precipitation scales exponentially with both GMST and the Niño3.4 index, as described in Section 2.3; the statistical model is fitted independently at each grid cell and each station for the period 1979-2023. The stations exhibit widely varying trends, with some stations along the coast and in the south of the catchment becoming somewhat wetter due to climate change, but stations further inland tending to become drier. CHIRPS reflects this pattern to some extent, with a slight wetting trend over the lake itself and along the northern coastline but drying elsewhere, while ERA5-Land and MSWEP both display a strong east-west gradient not seen in the stations. The effect of Niño3.4 is much more consistent over the region (Figure 3.4), having a drying effect over all grid cells and all stations, although of varying magnitudes.

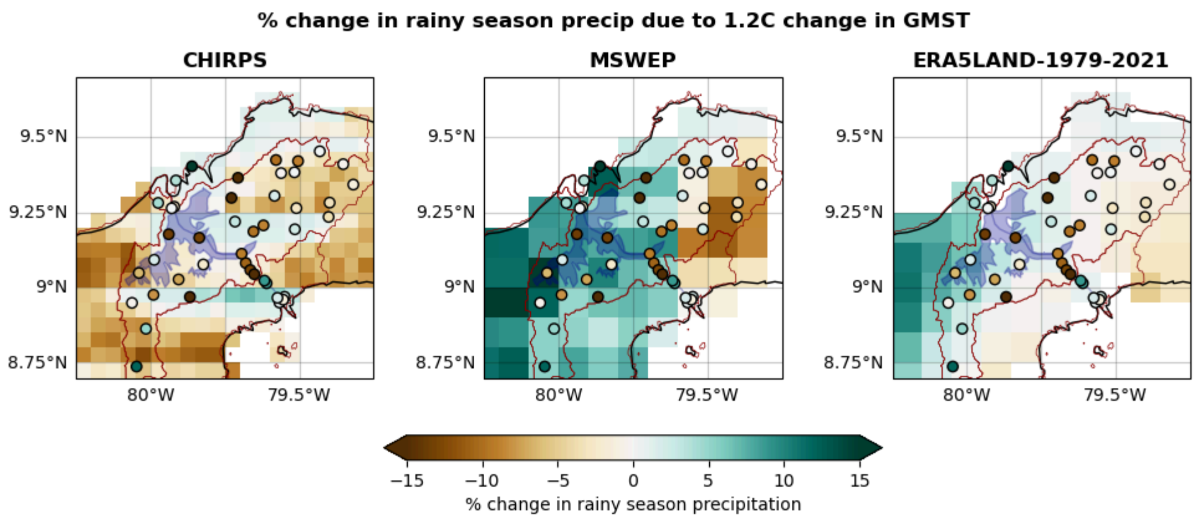

Figure 3.3 *Maps of expected % change in accumulated rainy season precipitation in response to a 1.2C increase in GMST, under a model in which rainy season precipitation increases exponentially with both GMST and detrended Niño3.4 index. Circles represent the expected % change in 43 ACP stations monitored by the ACP.*

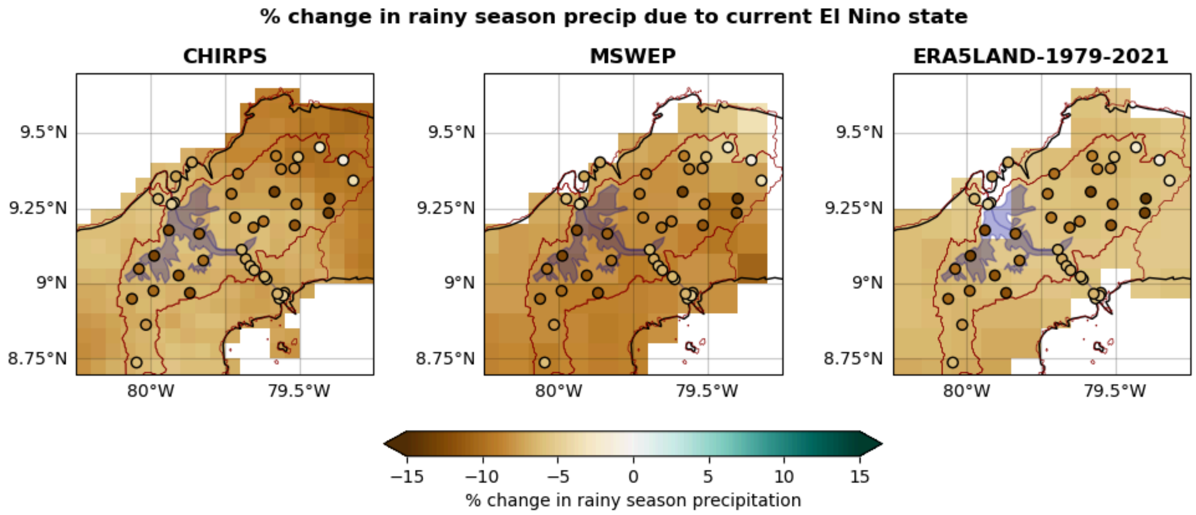

Figure 3.4: *Maps of expected % change in accumulated rainy season precipitation in response to the May-December 2023 mean of the detrended Nino3.4 index when compared to a neutral phase, under a model in which rainy season precipitation increases exponentially with both GMST and detrended Niño3.4 index. Circles represent the expected % change in 43 ACP stations monitored by the ACP.*

Finally, Figure 3.5 shows the time series of accumulated rainy-season precipitation averaged over the study region from 1979-2023, the period for which data is available in all of the time series. The effect of using longer time series to analyse the trends is explored using station data in Section 3.2.1.

Prior to 2023 the time series for the three gridded data products are broadly similar and highly correlated with the series obtained by averaging over the ACP stations. We retain all three of the gridded data products for trend analysis in Section 3.2, but disregard the 2023 observations for MSWEP and ERA5-Land when estimating the return period of the event. Furthermore, as well as very low values in 2022 and 2023, ERA5-Land has several extremely high values in the 1950s (not shown), which are not reflected in the available station data. In order to avoid introducing an artificial drying trend due to these anomalous values, we therefore only use ERA5-Land data from 1979-2021 to estimate the trend in rainy season precipitation. Because they fail to properly represent both the spatial pattern of precipitation trends and the 2023 precipitation deficit seen in the station data, neither MSWEP nor ERA5-Land is included in the final synthesis.

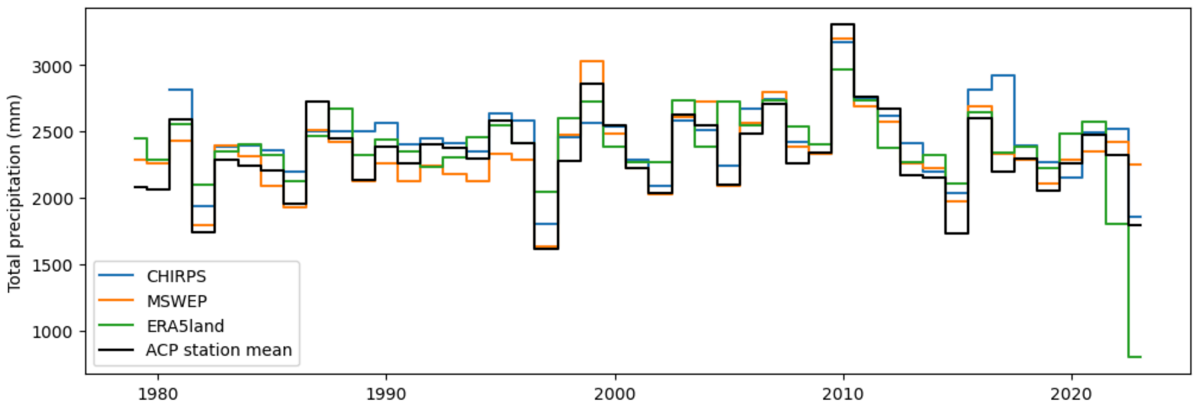

Figure 3.5: *Time series of accumulated rainy season precipitation (May-December) over the study region for the three gridded datasets and the ACP station series.*

3.2 Analysis of trends in precipitation

Figure 3.6 shows the time series of May-December precipitation averaged over the region and over a composite of the ACP stations shown in Figures 3.1 and 3.2. Only the period from 1979-2023 is plotted, but the model was fitted to the ACP station series from 1925-2023, so that the final synthesised result incorporates an estimate of the trend over a much longer time period. The sensitivity of the trend in the station data to the time period used is explored in Section A1; use of a longer time series produces slightly stronger evidence for a drying trend in this region. Despite the different time period used to estimate the model parameters, the fitted mean trends and 40-year return periods are similar.

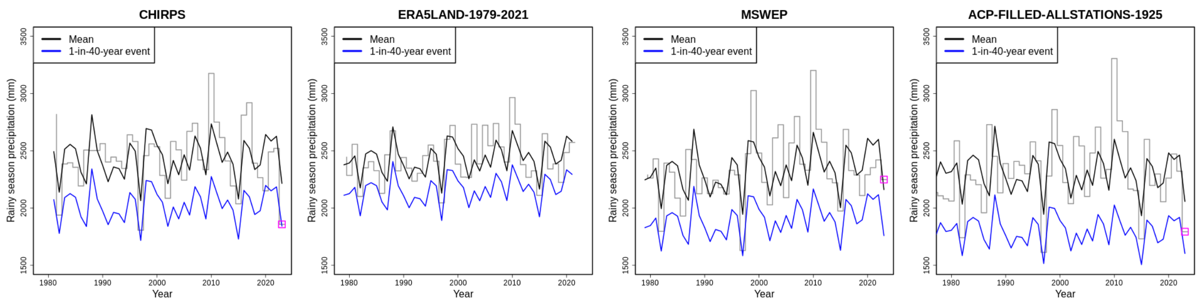

Figure 3.6: *Time series of accumulated rainy season precipitation over the study region for the three gridded datasets and the ACP station series. The pink dot marks the 2023 event; the heavy black line indicates the mean of the fitted model, and the blue line indicates the expected return levels of 40-year events. For easier comparison, only the years from 1979-2023 are plotted; however, the ACP station model is fitted to the reconstructed time series from 1925-2023.*

Figure 3.7 plots the fitted model against the GMST covariate with the Niño3.4 covariate fixed at its mean level (top row) and against the detrended Nino3.4 covariate with the GMST covariate fixed at its mean level (bottom row). In the gridded data products, all of which are fitted to the satellite period from 1979-2023, precipitation is largely independent of GMST, with CHIRPS having a weak drying trend and ERA5-Land and MSWEP a slight wetting trend. In the longer ACP time series, there is a somewhat stronger drying trend, which although still not statistically significant has a confidence interval that only just encompasses the possibility of no change (Table 3.1a): as shown in Section 3.2.1, similarly weak evidence of a drying trend is obtained regardless of the length of time series used. The effect of a positive ENSO phase on precipitation is much clearer, with all datasets showing clear evidence of lower precipitation in El Niño years: the current moderately positive state is associated with 6-8% less rain than in a neutral year (95% confidence intervals: 4-5% less to 8-11% less rain, Table 3.1b).

Table 3.1: *% change in intensity in each dataset corresponding to (a) a 1.2°C increase in GMST (b) the mean phase of the detrended Niño3.4 index during the 2023 rainy season. Figures in brackets define the central 95% confidence interval obtained by bootstrapping.*

	(a) GMST effect	(b) Niño effect
CHIRPS (1981-2023)	-3% (-12%, +8%)	-8% (-10%, -4%)
ERA5-Land (1979-2021)	+1% (-5%, +9%)	-6% (-8%, -4%)
MSWEP (1979-2023)	+4% (-5%, +15%)	-8% (-11%, -4%)
ACP stations (1925-2023)	-7% (-15%, 1%)	-8% (-11%, -5%)

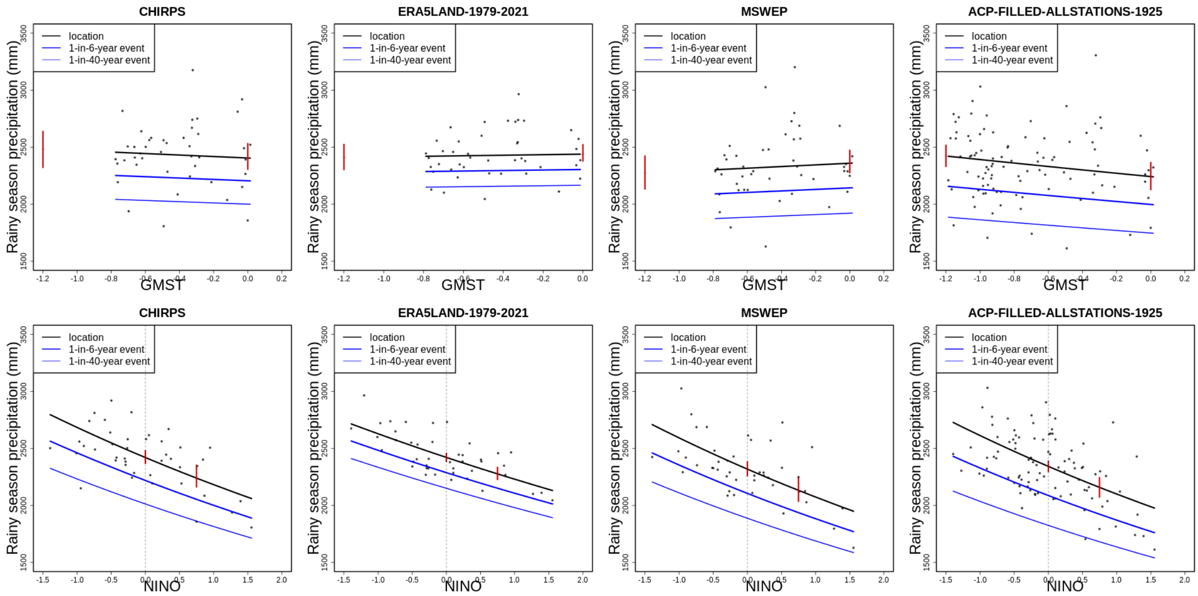

Figure 3.7: *Linear trend in accumulated rainy season precipitation over the study region as a function of GMST, with Niño3.4 held constant at the mean level (top row) and as a function of detrended Niño3.4 with GMST held constant at its mean level (bottom row). The thick black line denotes the location parameter of the fitted distribution, and the blue lines show estimated 6- and 40-year return levels. The 2023 observation is highlighted in magenta. Vertical lines show a bootstrapped confidence interval for the location parameter at (top row) the 2023 GMST and a 1.2°C cooler GMST; (bottom row) the 2023 Niño3.4 state and a neutral state.*

As noted in Section 3.1 above, ERA5-Land has extremely low precipitation in 2023, while MSWEP records the year as wetter than average, which we know not to be the case; we therefore do not present return periods for these two datasets. CHIRPS records 1857 mm of rain during the 2023 season, corresponding to a return period of 33 years in the current climate and under the current ENSO state (95% confidence interval: 10 to 1095), while the ACP station average is 1793mm, corresponding to a return period of 8 years (4, 28). Because we have no reason to prefer either CHIRPS or the station composite (which is not fully spatially representative of the region), we therefore assess this to be approximately a 20-year event in the 2023 climate and under the 2023 Niño3.4 conditions.

Table 3.2 shows the estimated factor increase in likelihood of experiencing a May-December rainfall deficit at least as extreme as that observed in 2023 due to (a) a 1.2°C increase in GMST and (b) the mean Niño3.4 state during the 2023 rainy season. Neither ERA5-Land nor MSWEP indicate any change in the probability of a similar event due to global warming, although our confidence in these products in this region is lower, as discussed in Section 3.1; in CHIRPS the event is around twice as likely, with a 95% confidence interval from 0.11 to 29.01; in the longer ACP station series, the event is around 3 times more likely, with a 95% confidence interval from 0.9 to 10 (column a). Again, the effect of El Niño on precipitation during the rainy season is clearer: for all of the datasets, the lower bound of the 95% confidence interval is greater than 1, indicating increased likelihood of low rainfall due to the current Niño3.4 state (column b). Taking into account the observed behaviour of Niño3.4 since 1900 following the method outlined in Section 2.3.2, rainy season deficits of similar magnitude to the 2023 event are expected to occur once every 63 years overall according to CHIRPS (95% confidence interval: 21-1100) and once every 16 years according to the ACP station mean (8-51).

Table 3.2: *Probability ratio (PR) in each dataset corresponding to (a) a 1.2°C increase in GMST (b) the mean phase of the detrended Niño3.4 index during the 2023 rainy season. Figures in brackets define the central 95% confidence interval obtained by bootstrapping.*

	(a) GMST effect	(b) Niño effect
CHIRPS (1981-2023)	2.11 (0.11, 29.01)	6.6 (3.1, 28.3)
ERA5-Land (1979-2021)	0.99 (0.93, 1.06)	1.17 (1.05, 1.45)
MSWEP (1979-2023)	0.83 (0.49, 1.32)	2.1 (1.55, 3.5)
ACP stations (1925-2023)	2.95 (0.87, 10.04)	3.16 (2.06, 5.67)

Figure 3.8 shows the modelled change in return levels due to a 1.2°C change in GMST from the preindustrial to the current climate. The points representing the rainfall recorded in each dataset lie within the shaded region indicating the 95% confidence interval indicating that the chosen statistical model fits the data well. In the gridded datasets there is no clear separation between the return levels in the current climate (red) and the past climate (blue), reflecting the small estimated effect of increased GMST on precipitation in the region.

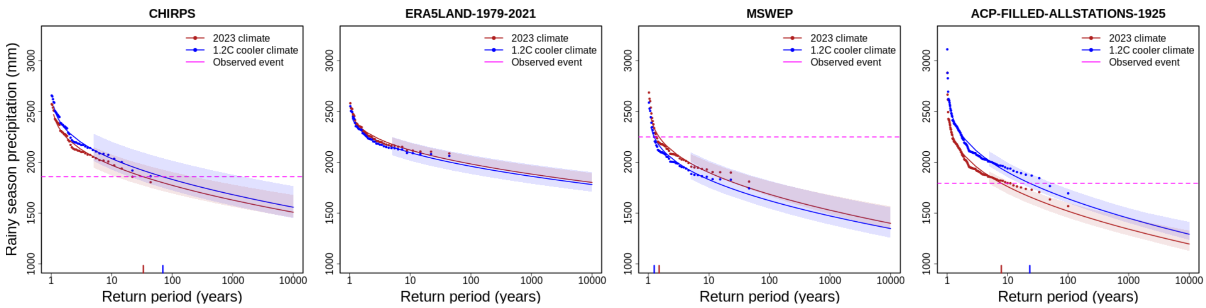

Figure 3.8: *Return levels for rainy season precipitation over the study region at the 2023 GMST (red lines) and 1.2°C lower GMST (blue line), with the Niño3.4 covariate fixed at its 2023 level. Shaded regions represent 95% confidence intervals obtained via a bootstrapping procedure. The pink line shows the accumulated precipitation during the 2023 rainy season. Red and blue ticks at the x axis indicate the estimated return level of the 2023 rainy season in the 2023 climate and 1.2°C cooler climate respectively.*

3.2.1 Effect of length of station time series on estimated trend

The results of the observational analysis in Section 3.2 use time series of gridded data from 1979-2023 to evaluate the contribution of both GMST and ENSO to the 2023 precipitation deficit, and a longer composite time series from 1925-2023 constructed by averaging infilled data from the ACP stations. To test the sensitivity of the results to this choice, we fitted the same statistical model both to longer and shorter time series, and to different subsets of the stations. The results of this analysis are shown in Figure 3.9. Each colour represents a different length of time series (beginning in 1881, 1900, 1925, 1950 and 1979); the model was fitted to the mean of all 44 ACP stations in the infilled dataset (darker bars), and also to the subset of stations for which relatively complete data was available before infilling (lighter bars). A station was deemed to have sufficiently complete data for inclusion in each subset if observations were available in more than 90% of the years in the period considered; maps of the selected stations for each time period can be found in Figure A1 in the Appendix.

Figure 3.9 shows that the key results - the return period of the 2023 season, probability ratio (PR) and relative change in intensity - are fairly robust to the choice of stations and the length of the time series considered. The best estimate of the return period in the 2023 climate is between around five and thirteen years; uncertainty about this value is lower in the subsets than when all stations are included, and somewhat higher in time series starting after 1950. In all of the samples there is some evidence of a drying trend associated with increased GMST, although the trend is significant only in the longer time series; this may be due to the difficulty of distinguishing the trend in GMST from multi-decadal variability in such short time series, or due to a systematic change in the location of the stations if, for example, more stations in areas with a wetting trend became active between 1925 and 1950. There is a much clearer effect from Niño3.4 across all of the time series tested, with 5-10% less precipitation predicted under the 2023 Niño3.4 conditions than in a neutral ENSO state, and similarly low precipitation expected around 2-5 times more often under the 2023 Niño3.4 conditions than in a neutral ENSO state. Given the consistency of the results across the subsets, we do not expect our conclusions to be sensitive to the length of time series used in the observational analysis.

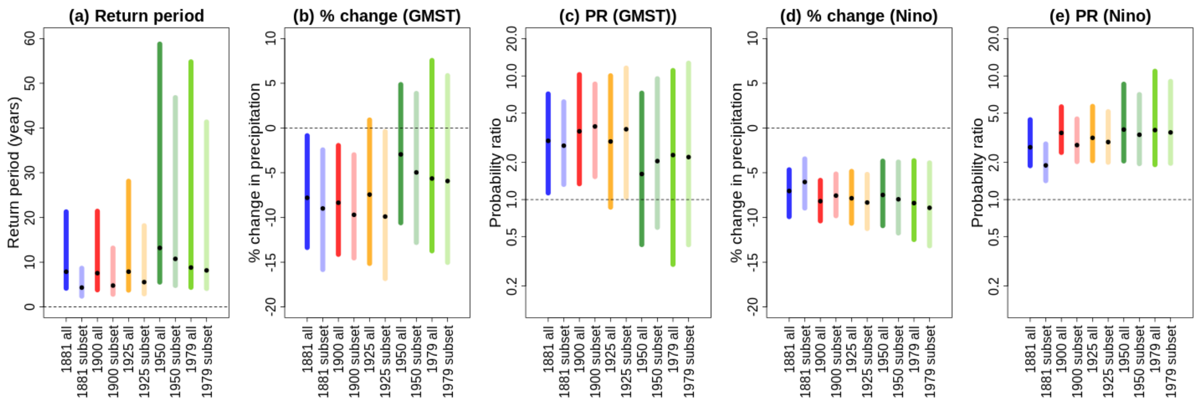

Figure 3.9: *Results of fitting the nonstationary GEV model to various subsets of the ACP station data: (a) return period of the 2023 low rainfall event; (b-c) relative change in intensity and probability ratio associated with 1.2°C increase in GMST; (d-e) relative change in intensity and probability ratio associated with the 2023 positive Niño3.4 phase.*

3.3 Trends in potential evapotranspiration

Water availability is affected not only by changes in precipitation but also by changes in evapotranspiration, which reduces the amount of effective rainfall. Observations of evaporation from close to ground level at the ACP station at Barro Colorado Island (BCI) are available for all months from 1991-2019; while this series is not long enough to reliably estimate a trend, the total annual evaporation over this period was around 950mm per year, with a standard error of ±100mm; around 450mm of this evaporation occurred during the dry season, and around 500mm during the wet season.

Data from an ACP study from 1996-2002 (not presented here) suggests that evapotranspiration in the region is strongly dependent on wind speeds, particularly during the dry season; for this reason, purely temperature-based estimates of potential evapotranspiration (PET) are unlikely to give an accurate picture of trends over recent decades. Instead, we here assess two gridded data products (ERA5-Land and TerraClimate) that provide estimates of PET using the Penman-Monteith equation (Monteith, 1965), which takes into account wind speed, humidity and solar radiation, as well as temperature. Time series of accumulated PET during both the wet and dry seasons, averaged across the study region for the two gridded data products, are shown in Figure 3.10 along with observed PET at BCI station. While we do not expect the gridded products to closely replicate the exact values observed at the station, this gives a useful indication of whether the gridded products are correctly representing the approximate mean level and variability of PET in the region.

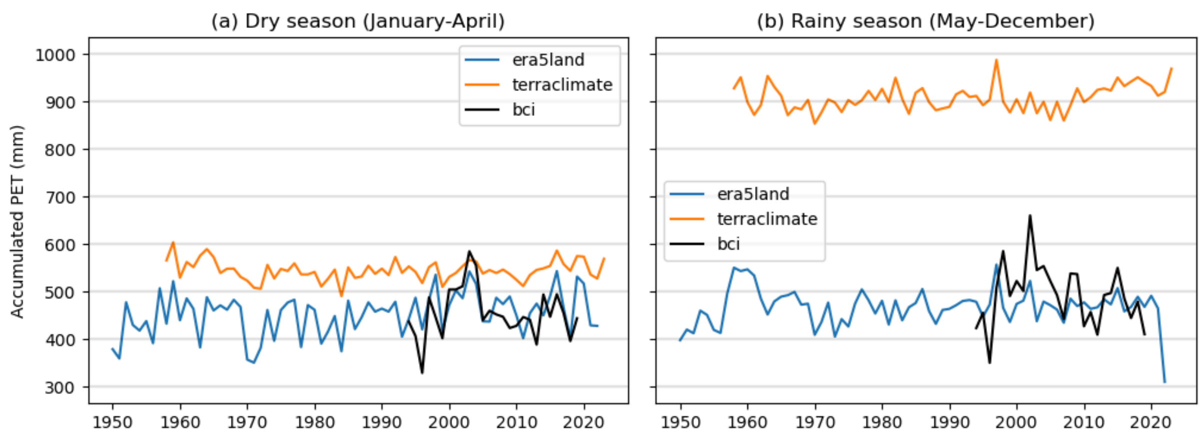

Figure 3.10: *Annual time series of accumulated evaporation averaged over the study region for ERA5-Land and TerraClimate, and from the ACP Claro station at Barro Colorado Island during (a) the dry season and (b) the rainy season. ERA5-Land values were divided by 4 before plotting.*

Neither of the gridded PET products can be used to support a full analysis of trends in PET. In order to appear on the same scale as the station data, ERA5-Land precipitation had to be divided by 4; the reason for this is not known, but we assume that this is an issue with unit encoding rather than the estimated values themselves, which are quite close to those observed at BCI station during both the dry and rainy seasons after this adjustment. At the time of writing, data were not available for 2023 in ERA5-Land; furthermore, the 2022 rainy season accumulation is extremely low. While TerraClimate estimates approximately the right level of PET during the dry season, the accumulation during the rainy season is clearly overestimated and interannual variability is low, further reducing our confidence in the data. We therefore do not attempt to estimate the return period of the 2023 PET or to estimate the effective precipitation by subtracting the PET from the corresponding rainfall time series. Instead, we fit a linear model in which PET shifts with both GMST and the detrended Niño3.4 index and use this to estimate the likely contribution from PET to reduced water availability during 2023. Separate models were fitted to dry season and rainy season PET, using the corresponding mean of the detrended Niño3.4 index as the second covariate to capture the potentially different processes affecting the two seasons.

In both ERA5-Land and TerraClimate there is some evidence of an increase in PET in both the dry and rainy seasons due to global warming (Table 3.3). From January-April 2023, this was offset somewhat by the effect of the declining negative (La Niña) phase, but slightly more PET was expected from May-December than in a neutral year, as the positive Niño phase began to strengthen. In total, ERA5-Land predicts around 89mm more PET (95% confidence interval: 8, 163) in the 2023 climate than in a preindustrial climate with a neutral Niño3.4 state, while TerraClimate predicts 57mm more (6, 103), with much of this increase driven by GMST, most likely through increasing local temperatures. Given that the 2023 precipitation deficit with respect to the 1990-2020 climatology was estimated to be around 400mm in CHIRPS and 700mm across the available stations, and that around half of the observed warming had already occurred by that period, these results suggest that increased PET due to global warming is unlikely to be a significant contributor to water shortages in the region. The remainder of this report therefore focuses on changes in precipitation only.

Table 3.3: *Expected change in accumulated PET (mm) during the dry and rainy seasons in each dataset corresponding to (a) a 1.2°C increase in GMST (b) the mean phase of the detrended Niño3.4 index during the 2023 dry and rainy seasons, and the expected change in overall annual accumulated precipitation. Figures in brackets define the central 95% confidence interval obtained by bootstrapping.*

	Dry season		**Rainy season**		
	GMST effect	**Niño effect**	**GMST effect**	**Niño effect**	**Total**
ERA5-Land	69 (33, 102)	-21 (-32, -11)	23 (-3, 47)	18 (10, 24)	89 (8, 163)
TerraClimate	15 (-4, 32)	-11 (-16, -6)	40 (18, 57)	14 (8, 20)	57 (6, 103)

4 Model evaluation

Climate models are evaluated against the CHIRPS and the ACP station composite for their ability to capture the distribution of rainy season precipitation in central Panama. The models are labelled as ‘good’ if the best estimate of each parameter (in this case, the dispersion of the fitted model and the correlation between rainy-season precipitation and the detrended Niño3.4 index) falls within the bounds estimated from the observations; ‘reasonable’ if the confidence interval for the model overlaps with the range estimated from the observations; or ‘bad’ if the ranges do not overlap. Models are also evaluated in terms of how well they represent the spatial and seasonal patterns of precipitation over the region. If the model is ‘good’ for all criteria, we give it an overall rating of ‘good’. In addition, models were rated as ‘bad’ if the 95% confidence interval for the change in intensity due to Niño3.4 included zero, since this indicates a failure to replicate the known relationship between El Niño events and low precipitation. Overall we rate each model as ‘reasonable’ or ‘bad’, if it is rated ‘reasonable’ or ‘bad’, respectively, for at least one criterion.
Table 4.1 shows the results of this model evaluation; because only three models were evaluated as ‘good’, models deemed ‘reasonable’ were also included in the final synthesis described in Section 5.

Table 4.1: *Evaluation of the climate models considered for attribution of rainy-season precipitation over central Panama. For each model, the best estimate of the dispersion parameters is shown, along with the correlation between rainy season precipitation and the detrended Niño3.4 index, and a 95% confidence interval for each, obtained via bootstrapping. The qualitative evaluation is shown in the right-hand column.*

Observations / Models	**Seasonal cycle**	**Spatial pattern**	**Dispersion**	**Correlation with Niño3.4**	**Overall**
chirps			0.0858 (0.0656 ... 0.0959)	-0.63 (-0.79 ... -0.37)	
acp-filled-allstations-1925			0.113 (0.0951 ... 0.128)	-0.50 (-0.64 ... -0.33)	
CAM-22_CanESM2 r1i1p1_CRCM5	bad	good	0.13 (0.10 ... 0.22)	-0.83 (-0.89 ... -0.77)	bad
CAM-22_CNRM-CM5 r1i1p1_CRCM5	good	good	0.10 (0.080 ... 0.11)	-0.29 (-0.47 ... -0.086)	reasonable
CAM-22_GFDL-ESM2M r1i1p1_CRCM5	good	good	0.12 (0.088 ... 0.20)	-0.85 (-0.90 ... -0.77)	reasonable
CAM-22_GFDL-ESM2M r1i1p1_RegCM4-7	good	good	0.080 (0.053 ... 0.10)	-0.75 (-0.84 ... -0.63)	good
CAM-22_HadGEM2-ES r1i1p1_RegCM4-7	reasonable	good	0.12 (0.090 ... 0.13)	-0.68 (-0.77 ... -0.58)	reasonable
CAM-22_HadGEM2-ES r1i1p1_REMO2015	good	good	0.089 (0.062 ... 0.11)	-0.062 (-0.28 ... 0.15)	bad
CAM-22_MPI-ESM-LR r1i1p1_REMO2015	good	good	0.16 (0.12 ... 0.19)	-0.16 (-0.42 ... 0.19)	bad
CAM-22_MPI-ESM-MR r1i1p1_RegCM4-7	good	reasonable	0.13 (0.089 ... 0.15)	-0.67 (-0.79 ... -0.51)	reasonable
CAM-22_NorESM1-M r1i1p1_REMO2015	bad	good	0.41 (0.18 ... 0.52)	-0.85 (-0.91 ... -0.74)	bad
CAM-44_CanESM2 r1i1p1_CRCM5	bad	good	0.17 (0.14 ... 0.30)	-0.81 (-0.88 ... -0.73)	bad
CAM-44_CanESM2 r1i1p1_RCA4	reasonable	good	0.24 (0.18 ... 0.28)	-0.61 (-0.71 ... -0.48)	bad
CAM-44_CNRM-CM5 r1i1p1_RCA4	good	good	0.097 (0.070 ... 0.11)	-0.45 (-0.60 ... -0.27)	good
CAM-44_CSIRO-Mk3-6-0 r1i1p1_RCA4	reasonable	reasonable	0.41 (0.34 ... 0.61)	-0.66 (-0.79 ... -0.51)	bad
CAM-44_GFDL-ESM2M r1i1p1_RCA4	good	good	0.17 (0.12 ... 0.26)	-0.84 (-0.90 ... -0.75)	reasonable
CAM-44_HadGEM2-ES r1i1p1_RCA4	good	good	0.085 (0.063 ... 0.099)	-0.52 (-0.66 ... -0.35)	good
CAM-44_IPSL-CM5A-MR r1i1p1_RCA4	reasonable	good	0.22 (0.16 ... 0.25)	-0.34 (-0.56 ... -0.070)	bad
CAM-44_MIROC5 r1i1p1_RCA4	good	good	0.33 (0.15 ... 0.38)	-0.85 (-0.89 ... -0.79)	bad
CAM-44_MPI-ESM-LR r1i1p1_RCA4	good	reasonable	0.13 (0.099 ... 0.15)	-0.56 (-0.71 ... -0.38)	reasonable
CAM-44_NorESM1-M r1i1p1_RCA4	reasonable	good	0.17 (0.14 ... 0.36)	-0.84 (-0.91 ... -0.74)	bad
SAM-22_HadGEM2-ES r1i1p1_RegCM4-7	reasonable	bad	0.19 (0.15 ... 0.22)	-0.43 (-0.62 ... -0.22)	bad

SAM-22_HadGEM2-ES r1i1p1_REMO2015	good	reasonable	0.072 (0.052 ... 0.083)	0.21 (-0.054 ... 0.46)	bad
SAM-22_MPI-ESM-LR r1i1p1_REMO2015	good	reasonable	0.13 (0.097 ... 0.16)	-0.087 (-0.34 ... 0.23)	bad
SAM-22_MPI-ESM-MR r1i1p1_RegCM4-7	good	bad	0.21 (0.15 ... 0.23)	-0.56 (-0.74 ... -0.33)	bad
SAM-22_NorESM1-M r1i1p1_RegCM4-7	bad	reasonable	0.37 (0.26 ... 0.43)	-0.63 (-0.81 ... -0.35)	bad
SAM-22_NorESM1-M r1i1p1_REMO2015	reasonable	reasonable	0.20 (0.15 ... 0.36)	-0.79 (-0.89 ... -0.64)	bad
SAM-44_CanESM2 r1i1p1_RCA4	bad	reasonable	0.099 (0.072 ... 0.12)	-0.31 (-0.53 ... -0.056)	bad
SAM-44_CNRM-CM5 r1i1p1_RCA4	good	reasonable	0.063 (0.050 ... 0.076)	-0.46 (-0.54 ... -0.37)	reasonable
SAM-44_CSIRO-Mk3-6-0 r1i1p1_RCA4	bad	reasonable	0.14 (0.12 ... 0.15)	-0.62 (-0.72 ... -0.52)	bad
SAM-44_GFDL-ESM2M r1i1p1_RCA4	good	reasonable	0.11 (0.10 ... 0.13)	-0.48 (-0.66 ... -0.43)	reasonable
SAM-44_HadGEM2-ES r1i1p1_RCA4	reasonable	reasonable	0.066 (0.052 ... 0.074)	-0.46 (-0.59 ... -0.38)	reasonable
SAM-44_IPSL-CM5A-MR r1i1p1_RCA4	bad	reasonable	0.11 (0.093 ... 0.13)	-0.55 (-0.66 ... -0.46)	bad
SAM-44_MIROC5 r1i1p1_RCA4	reasonable	reasonable	0.095 (0.074 ... 0.097)	-0.66 (-0.71 ... -0.52)	reasonable
SAM-44_MPI-ESM-LR r1i1p1_RCA4	good	reasonable	0.077 (0.060 ... 0.088)	0.16 (0.022 ... 0.30)	bad
SAM-44_MPI-ESM-LR r1i1p1_REMO2009	good	bad	0.11 (0.088 ... 0.12)	-0.17 (-0.25 ... 0.027)	bad
SAM-44_NorESM1-M r1i1p1_RCA4	reasonable	reasonable	0.097 (0.079 ... 0.17)	-0.76 (-0.84 ... -0.68)	reasonable

5 Multi-method multi-model attribution

Table 5.1 shows probability ratios (PR) and changes in intensity (ΔI) for the observational data products and for and for those models that passed the evaluation described in Section 4.

Table 5.1: *Event magnitude, probability ratio and relative change in intensity for 20-year low rainy season precipitation over central Panama for observational datasets and each model that passed evaluation: (a) from the preindustrial climate to the present and (b) from the present to 2°C above preindustrial.*

		(a) -1.2°C vs present		(b) Present vs +0.8°C	
Model / Observations	**20-year event (mm)**	**Probability ratio**	**Change in intensity (%)**	**Probability ratio**	**Change in intensity (%)**
chirps	1857	2.1 (0.11 ... 29)	-3.2 (-12 ... 8.2)		

acp-filled-allstations-1925	1793	2.9 (0.87 ... 10)	-7.4 (-15 ... 0.90)		
CAM-22_CNRM-CM5 r1i1p1_CRCM5	1877	1.0 (0.26 ... 4.4)	-0.0072 (-8.3 ... 7.8)	1.0 (0.36 ... 2.2)	-0.0048 (-5.9 ... 4.9)
CAM-22_GFDL-ESM2M r1i1p1_CRCM5	1843	0.75 (0.23 ... 2.7)	1.9 (-6.1 ... 9.6)	0.82 (0.32 ... 1.8)	1.3 (-4.3 ... 6.0)
CAM-22_GFDL-ESM2M r1i1p1_RegCM4-7	1952	0.65 (0.094 ... 4.2)	2.1 (-5.0 ... 11)	0.74 (0.13 ... 2.1)	1.4 (-3.5 ... 6.9)
CAM-22_HadGEM2-ES r1i1p1_RegCM4-7	3073	0.99 (0.36 ... 3.7)	0.043 (-8.5 ... 7.2)	1.0 (0.48 ... 2.0)	0.029 (-6.1 ... 4.5)
CAM-22_MPI-ESM-MR r1i1p1_RegCM4-7	1963	3.8 (1.1 ... 52)	-9.3 (-20 ... -1.0)	2.2 (1.1 ... 5.9)	-6.7 (-16 ... -0.70)
CAM-44_CNRM-CM5 r1i1p1_RCA4	2009	1.6 (0.38 ... 9.8)	-2.6 (-11 ... 4.8)	1.4 (0.49 ... 3.1)	-1.8 (-8.2 ... 3.1)
CAM-44_GFDL-ESM2M r1i1p1_RCA4	1409	0.29 (0.082 ... 0.77)	16 (3.9 ... 31)	0.40 (0.15 ... 0.84)	9.7 (2.5 ... 17)
CAM-44_HadGEM2-ES r1i1p1_RCA4	3153	0.66 (0.21 ... 1.3)	2.5 (-1.4 ... 8.5)	0.75 (0.30 ... 1.2)	1.6 (-0.92 ... 5.3)
CAM-44_MPI-ESM-LR r1i1p1_RCA4	2222	0.97 (0.31 ... 3.1)	0.27 (-7.7 ... 8.2)	0.98 (0.43 ... 1.9)	0.18 (-5.5 ... 5.1)
SAM-44_CNRM-CM5 r1i1p1_RCA4	3983	0.95 (0.16 ... 1.9)	0.16 (-1.9 ... 5.1)	0.97 (0.21 ... 1.5)	0.11 (-1.3 ... 3.2)
SAM-44_GFDL-ESM2M r1i1p1_RCA4	3650	0.23 (0.070 ... 0.33)	12 (7.0 ... 22)	0.30 (0.083 ... 0.42)	7.1 (4.4 ... 12)
SAM-44_HadGEM2-ES r1i1p1_RCA4	5746	0.14 (0.044 ... 0.45)	9.0 (4.0 ... 11)	0.14 (0.038 ... 0.51)	5.6 (2.6 ... 6.7)
SAM-44_MIROC5 r1i1p1_RCA4	4632	0.19 (0.062 ... 0.32)	13 (7.0 ... 19)	0.25 (0.060 ... 0.41)	7.8 (4.4 ... 11)
SAM-44_NorESM1-M r1i1p1_RCA4	2584	0.23 (0.065 ... 0.23)	10 (9.5 ... 18)	0.30 (0.086 ... 0.29)	6.2 (5.9 ... 10)

6 Hazard synthesis

We now evaluate the evidence for the influence of anthropogenic climate change in rainy season precipitation over central Panama by calculating the probability ratio and change in intensity for both observations and climate models. Models which do not pass the validation tests described in Section 4 are excluded from the analysis. The aim is to synthesise results from models that pass the evaluation along with the observation-based products, to give an overarching attribution statement. Figure 6.1 shows the changes in probability and relative intensity of a 1-in-20-year event associated with an increase of 1.2°C in GMST in both the observations (light blue) and models (light red). The best estimate for each dataset is marked with a black triangle. A term to account for intermodel spread is added in quadrature to the natural variability of the models: this is shown in the figures as white boxes around the light red bars. The dark red bar shows the model average, consisting of a weighted mean using the (uncorrelated) uncertainties due to natural variability plus the term representing intermodel spread (the white bars). Observation-based products and models are combined into a single result in two ways. Firstly, we neglect common model uncertainties beyond the intermodel spread already incorporated in the model average, and compute the precision-weighted average of models (dark red bar) and observations (dark blue bar): this weighted mean is indicated by the magenta bar. To account for the fact that, due to common model uncertainties, model uncertainty can be larger than the intermodel spread, we also show an unweighted direct average of observations (dark blue bar) and models (dark red bar) contributing 50% each, indicated by the white box in the synthesis figures.

As discussed in Section 3.2, both CHIRPS and the ACP station composite show a slightly increased likelihood of low precipitation due to climate change and a corresponding reduction in accumulated rainy season precipitation although neither change is statistically significant (Figure 6.1, blue bars). The behaviour of the regional climate models is largely determined by the domain: models run over the Central America (CAM) domain tend to simulate no change in this region, while most of those using the South America domain simulate a drying trend. The reasons for this have not been examined, but we hypothesise that the Central America domain, which has Panama close to its centre, is better able to represent the northerly trade winds that affect the region's precipitation (Alfaro, 2002); conversely, the South American (SAM) domain includes the Amazon rainforest, which affects the water cycle in the wider region, but because Panama lies close to the northern edge of the domain, the contribution from the trade winds is unlikely to be properly represented. By retaining all of the models in the synthesis we capture the uncertainty about the contribution of each of these processes, which is reflected in the white boxes around the red bars; overall, the models simulate a slightly reduced likelihood of similar events due to climate change, and a slight increase in rainy-season precipitation. The overall conclusion is that, although the observations show a drying trend, when both observations and climate models are taken into account there is no evidence that the reduced rainy season precipitation in this region is attributable to anthropogenic climate change: the synthesised best estimate of the change in the likelihood of a season as dry as that experienced in 2023 is a factor of 0.91 (95% confidence interval: 0.26 to 3.1 times as likely), and the best estimate of the change in intensity is a reduction of 0.6% in precipitation from the preindustrial climate (95% confidence interval: ±8%). Similar results were obtained for projections of future changes in precipitation in the region under a further 0.8°C of warming (Figure 6.2). Unlike in cases where increasing water shortages are known to be driven by high evaporation that increases in a warming climate, further research is needed to understand the mechanisms driving reduced rainfall in this region and whether they are linked to global warming. This result is in accordance with the existing literature, which shows mixed trends in rainfall across Panama and Central America more widely depending on region, season and drought metrics used.

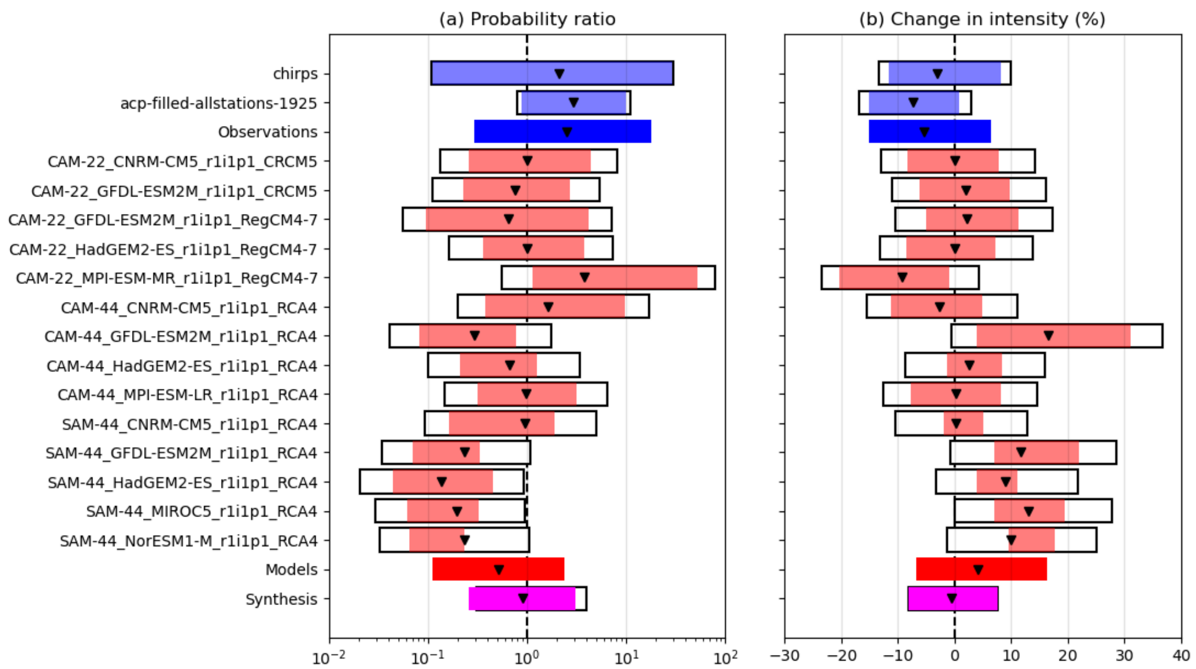

Figure 6.1: *Synthesis of (a) probability ratios and (b) relative intensity changes of expected May-December precipitation in the study region in the 2023 climate and a 1.2°C cooler climate. Details of how to interpret the synthesis plots are given in the text.*

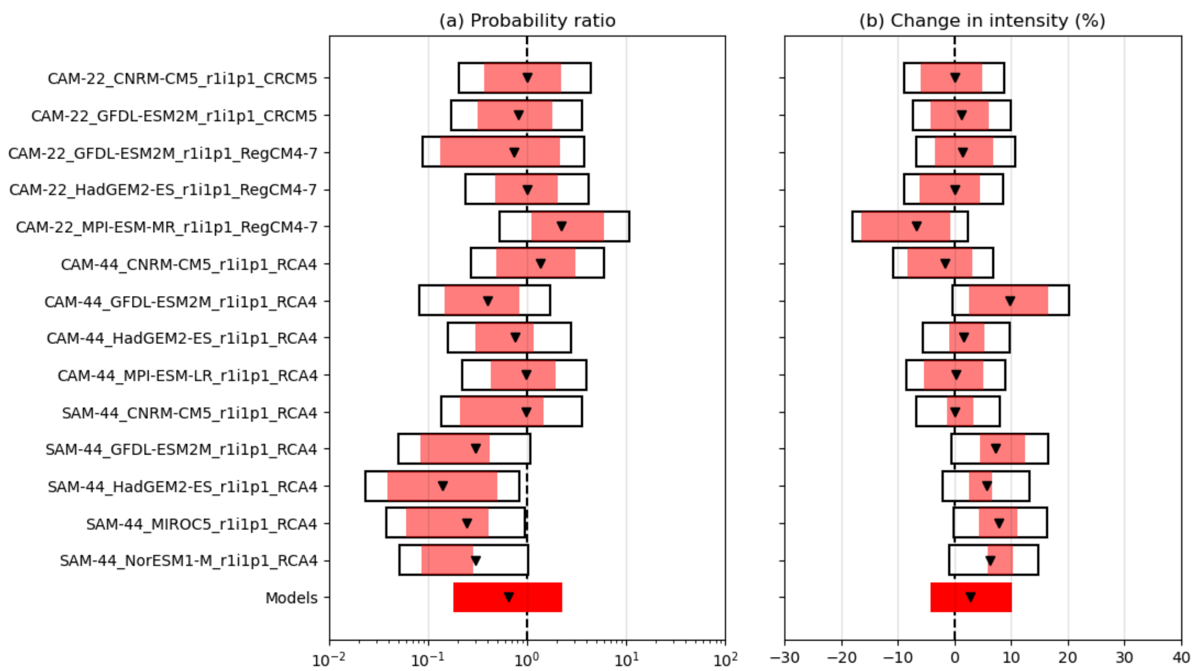

Figure 6.2: *Similar to Fig 6.1 but comparing a 0.8°C warmer climate (ie. after a total of 2°C of warming) to the 2023 climate, for models only.*

7 Vulnerability and exposure

Disaster risk is defined as the product of hazard, vulnerability, exposure, and coping capacity ([Cardona, 2012](#)). As such, this section complements the preceding hazard analysis for understanding the drivers at play in the materialization of impacts associated with the rainfall deficits. While impacts are yet to match the heights of the 2015/16 event, when Gatún Lake hit record low water levels and drinking water rationing was introduced, the 2023/24 event is unique because of how early the Panama Canal Authority (Autoridad del Canal de Panamá, ACP) was forced to respond.

It is important to note that existing reports on impacts primarily center on the national and global economy, with little focus on surrounding communities and people dependent on the Panama Canal Watershed (PCW), despite housing over half of Panama's population and the majority of its industries and services (National Water Council, 2015; Moloney, 2024). The Pacific slope, inhabited by some 83% of Panama's population, also harbours the highest demand for water (National Water Council, 2015). This area is the focal point for over 70% of the country's economic activities and includes the Metropolitan region, encompassing districts like Panama City, San Miguelito, La Chorrera, Arraiján, and Capira. These figures are forecasted to rise as this country's projected urban population growth is projected to increase by 12.5% to 4.6 million in 2050 compared to 2015 (ibid), putting greater pressure on Panama Canal's municipal water demand if resilience is not improved (Moloney, 2024).

The vulnerability and exposure analysis offers insight into the key factors that underpin the consequences on local communities, affected sectors, and the global economy. Specifically, it centers on four themes: water management, land-use changes, differential vulnerabilities, and global shipping. Identifying the drivers of risk and impact is pivotal for developing holistic strategies to mitigate the same for future periods of low rainfall in the PCW. However, further research and evaluation of response efforts will be essential to learn from the event.

7.1 Balancing water interests between the canal and municipal use

7.1.1 Water management

Panama is one of the world's most water-rich nations with water being a critical asset to this country's socio-economic development, flagshipped by Panama Canal. The Panama Canal utilises the reservoirs of Lake Gatún, established in 1910, and Lake Alhajuela, established in 1935 (Figure 1) (Gobbetti, 2017). Effective water management between Lake Gatún and Lake Alhajuela plays a significant role in maintaining Canal operations. When water levels drop in the shallower Gatún Lake, water is transferred from the deeper Alhajuela Lake (Predko, 2024). Led by the ACP and involving communities living on the PCW, Panama Canal's integrated water management system helped maintain waterway levels of over 13.72m during the 2020 dry season and into 2021 after Panama faced its fifth driest year in 70 years in 2019 (UNDP, 2020; ACP, 2021). Some of these measures include the preservation and restoration of the surrounding tropical forests, such as through incentivising small-scale PCW farmers, to reduce soil erosion, enhance water flow and improve water retention and storage (Moloney, 2024), initiatives that are currently in place. Intended to reduce the possibility of shipping restrictions, in 2020, the launch of the freshwater fee and additional conservation actions to the Canal's water management system further aided waterway levels (ACP, 2021). Nonetheless, the water management system has not been able to cope with the current rainfall deficits causing ACP to reduce the Canal's ship transit by up to 36%. On January 1st 2024, the canal's lowest water levels on record were monitored at some 6 feet lower than those a year prior due to rainfall deficits fuelled by extreme weather events as the canal's hydrological basin encountered one of its two driest years since records began in 1880 (Ruiz & Shintani, 2024; Moloney, 2024).

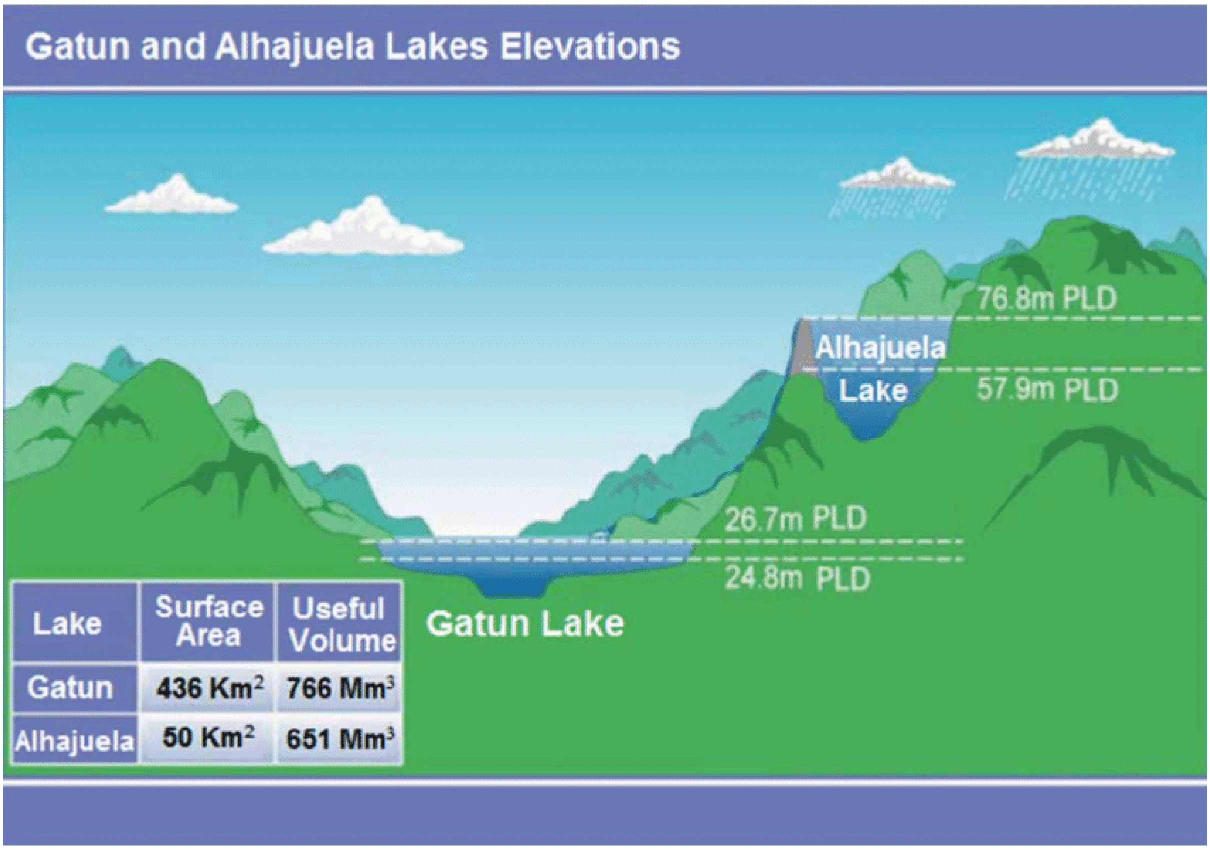

Figure 7.1: *Lake Alhajuela and Lake Gatún (ACP, 2006)*

In addition to being a major water source for global shipping transit, the Panama Canal watershed supplies some 55% of Panama's total population needs (Ruiz & Shintani, 2024), including 95% of the safe drinking water for several of Panama's largest population centres, including Panama City, Colón, San Miguelito and, as planned, for La Chorrera as well (National Water Council, 2015). Of the 119.5 billion cubic metres of freshwater, an estimated 30.3% was consumed in 2020 (ibid). The Canal's water consumption can be separated into non-consumptive and consumptive use. Non-consumptive use includes hydroelectric operation that requires 89.6% of water consumption, Panama Canal activity utilising 7.4%, and 0.01% for aesthetic purposes (ibid). Consumptive water usage accounts for the 1.7% used within agricultural practice, 1.3% for human consumption, 0.2% for industrial use and 0.01% for recreational tourism (ibid). Projections show water demand will increase more than double by 2050 compared to 2015 levels, potentially putting a strain on water security (ibid). At the same time, roughly 42% of the potable water produced is lost, due mostly to leaks, which suggests infrastructural opportunities for improvements in the water distribution system. These improvements could complement or altogether replace the plans on creating additional water reservoirs (Kingdom of the Netherlands, 2018).

With such a key resource and interoceanic infrastructure leading Panama's water-dependent economy and helping facilitate global shipping, Panama Canal's water management plans, conducted by the ACP, are crucial to its ability to ensure water security, socio-economic development and international trade. These plans, outlined within the National Water Security Plan 2015-2050: Water For All and co-ordinated by the National Water Council (CONAGUA), foreground the short-, medium- and long-term actions to protect Panama's water resources, aiming to enhance quality of life, promote inclusive socio-economic growth and improve water security (National Water Council, 2015). The National Water Security Plan 2015-2050 was devised by the Ministries of Health and Environment, National Public Services Authority and other relevant governmental bodies due to the effects of the extensive 2015 drought event on Panama, including on Panama Canal, which caused major water and energy shortages (ibid). After such impacts, this new plan took over the previous National Integrated Water Resources Management Plan 2010-2030 in 2015 (Cervera, 2018).

Panama's other surface and groundwater resources face many threats affecting settlements and wildlife habitats, such as aquifer contamination from increased salt-water intrusion and coastal erosion due to sea-level rise (Panama Aquatic Resources Authority, 2019). These threats are exacerbated by upstream pollution, including agricultural runoff, deposited in Panama's waters (Greaney, 2015). In addition to the low rainfall, the communities and wildlife habitats surrounding the Panama Canal have been extensively affected.

In addressing Panama's water security and alleviating the effects of water scarcity, improved management and storage of surplus water during wet seasons and years is imperative (Netherlands Water Partnership, 2022). Some of the ways to increase resilience evolve from the ACP accessing alternative water sources through desalination technology, circular use of water, dam, reservoir and river-flow management, storm-water management, and improved groundwater management and monitoring, for example, in addition to improved land-use management practices (ibid).

7.1.2 Expansion plans

Waterway experts, collaborating with the US Army Corps of Engineers (USACE), determined that the technical solutions possible within the Panama Canal's jurisdiction would be inadequate to satisfy the increasing water demand (ACP, 2023). Therefore, the potential solutions that would need to be pursued extend beyond the boundaries of Panama Canal and involve determining 'new' water sources (ibid). As part of the National Water Security Plan 2015-2050, consultations to identify 'new' sources of water occurred between 2017-2020 over the Indio River, Bayano River, Santa María River, La Villa River, Parita River and Pareles River to assess the feasibility of, for example, multipurpose reservoirs to strengthen water security and reduce stress on the Panama Canal drainage basin (ACP, 2021).

The construction of a new reservoir proposed on the Indio River (Figure 2) would require an estimated $900 million to complete over five years (Schexnayder, 2024). Due to the proposed reservoir location being on deforested land predominantly used for subsistence farming, this project is deemed to have a low environmental impact (Gobbetti, 2017). Nonetheless, the new reservoir construction would bring socio-economic and environmental repercussions for the communities living and working within its expanse and could displace thousands of farmers in the areas to be flooded (Livingstone, 2022). Thus, some communities living on the PCW oppose the proposed development (Moloney, 2024). Moreover, the project adds to the existing public dissatisfaction regarding environmental concerns, community rights, and the lack of policies to aid, for instance, poverty reduction (Harkins, 2024; Moloney, 2024).

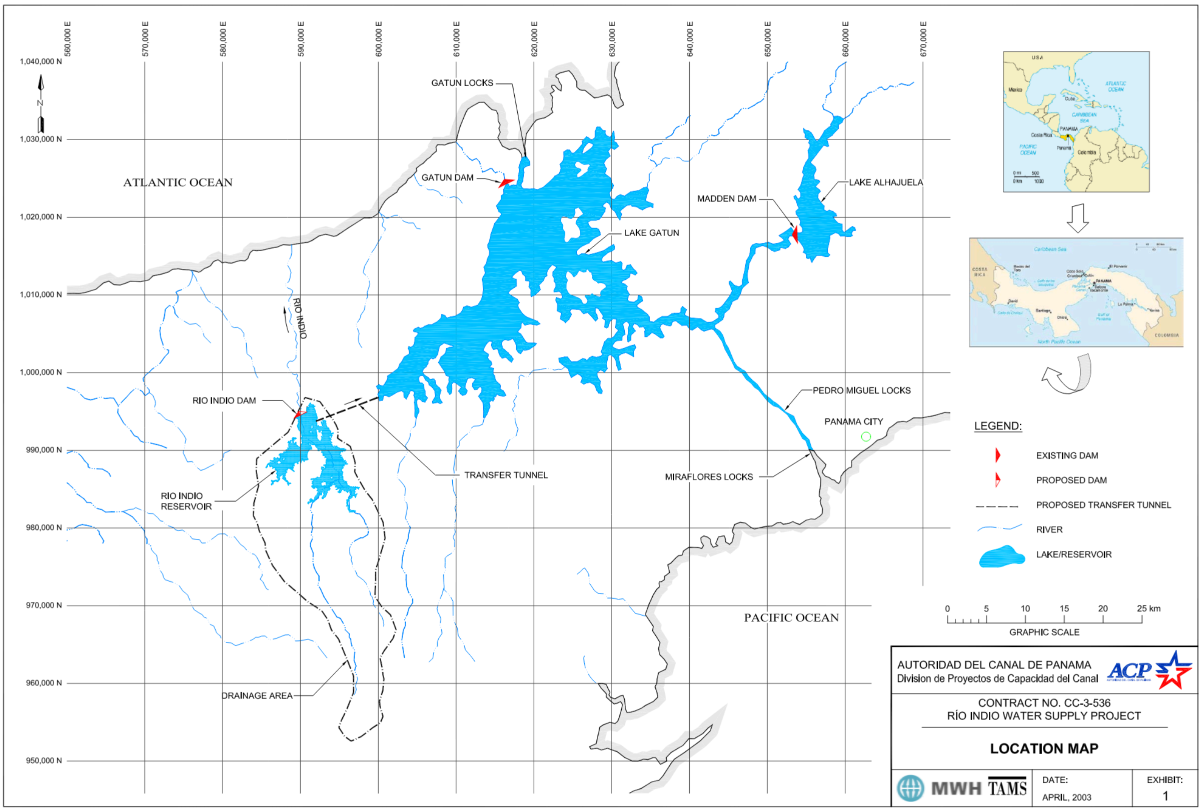

Figure 7.2: *Indio River Project Proposal Plans (Harza, 2003)*

Additional projects proposed include the Alto Chagres Project, hosting considerable hydroelectric potential, this undertaking involves building a new reservoir directly upstream from Alhajuela Lake (Figure 3) (Gobbetti, 2017). Furthermore, the Trinidad project involves constructing an underwater filling dam to isolate the Trinidad arm, a section of Lake Gatún, from its main body to enable surplus water from Lake Gatún to be supplied to the Trinidad arm during rainy periods (May-December) to utilize its supplementary storage capacity (Gobbetti, 2017). As already noted in the proposed Indio River Project, these strategies would also pose socio-economic and environmental impacts on those inhabiting and working on the land (Moloney, 2024). This could potentially escalate pre-existing public tensions (ibid), and will have to be considered and resolved during negotiations.

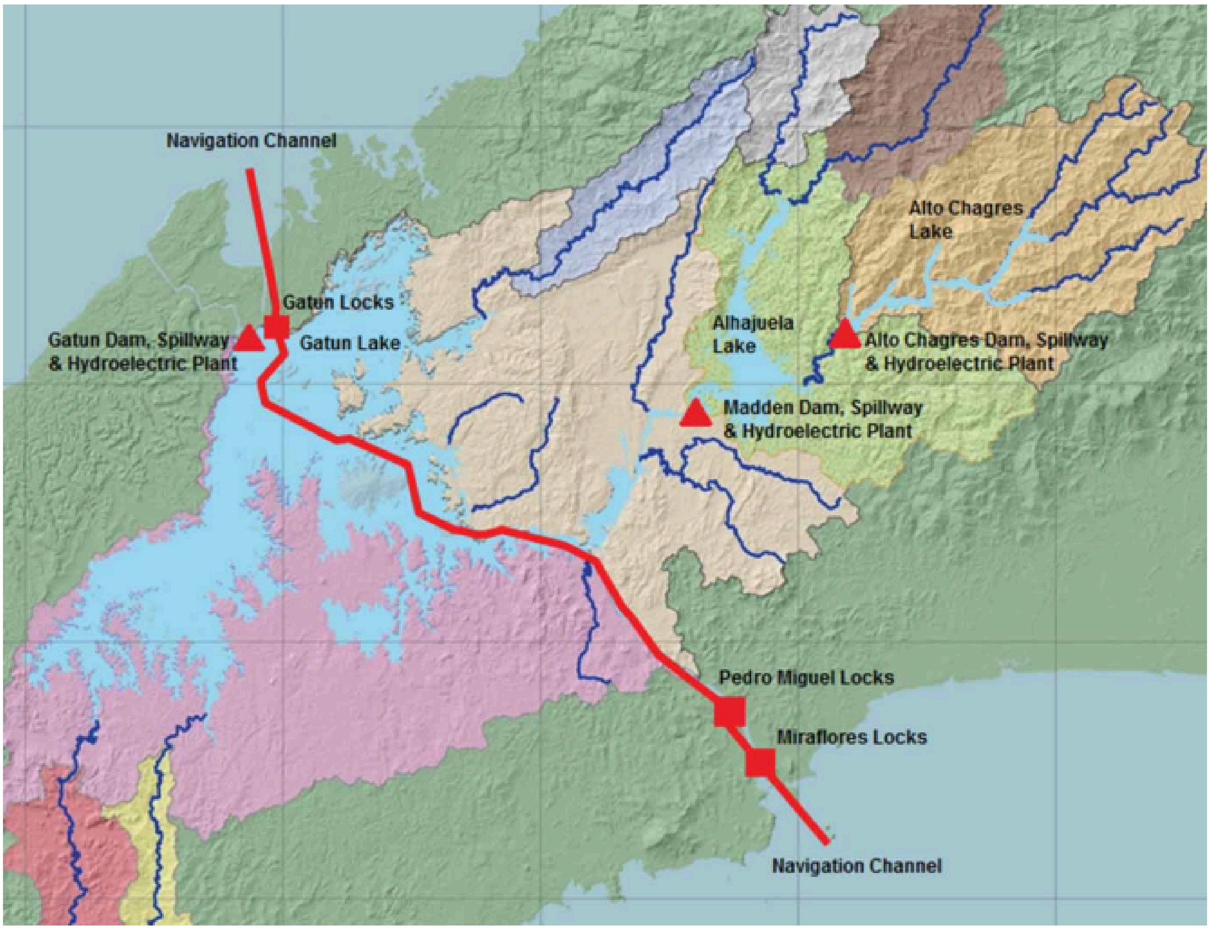

Figure 7.3: *Alto Chagres Project Proposal Plans (Gobbetti, 2017)*

7.2 Land-use changes and environmental degradation

The PCW spans 5,527 km², making up 6.5% of the country (Castro, n.d.). Eight protected natural areas of about 1,366 km², home to between 41 and 67% of the country's biodiversity, are spread across this vast territory (Ibánez et al., 2002). The Panama Canal is in the midst of Panama's rainforests, both dependent on precipitation for survival.

Over the past century, human settlement and activity within the PCW have left a significant imprint on its land cover. Between 1947 and 2014, Panama experienced a significant loss of forest cover, totalling 6.7 million acres, primarily attributed to ranching and agriculture activities (Silverstein, 2023). While difficult to ascertain because of changes to the methodology in estimating forest cover, Global Forest Watch (n.d.) suggests that the rate of net deforestation over the past 20 years has decreased. Today, this watershed not only meets the vital need of providing potable water to Panama City and Colón (ACP, n.d.), two major urban centres, but it also houses over half of the nation's population. The canal's reservoirs are the backbone of a sprawling metropolitan region that is currently home to an estimated two million people. The watershed provides the nearby cities of Panama City and Colón with essential municipal water and hydropower (Moreno, 2018). Beyond urban life, it sustains suburban communities and supports various agricultural, ranching, and forestry activities, highlighting its multifaceted importance in the fabric of Panamanian society (Dale et al., 2005).

7.2.1 Regional development plan

To address the multifaceted challenges posed by regional development and climate change within the Panama Canal river basin, the ACP has initiated the development of a comprehensive land use plan. This plan, guided by the Green Pathway 2050 roadmap, aims to ensure water security for the population, foster socio-economic development, maintain the reliable operations of the Panama Canal, and safeguard the ecosystem services of the basin (ACP, 2022).

The Indicative Environmental Land Use Plan (PIOTA) for the PCW developed through cooperation with the Inter-American Development Bank (IDB), began with a comprehensive diagnosis of the Watershed and analysis of trends and scenarios on the availability of water resources in the future (Future Water, 2020). This process sought socio-environmental commitment for the sustainable management of the PCW, through integrated management of the territory with a regional vision, including ecosystems and protected areas, with a focus on decarbonisation, resilience to climate change and disasters, allowing for the conservation of the resource and improving existing socioeconomic conditions (Idom, 2022).

The PIOTA provides a guiding framework for the sustainable and integrated management of the PCW over the next 50 years, outlining approaches to address issues such as outdated land-use and zoning practices, lack of urban planning, increased informal settlements in high risk areas and the unplanned expansion of agricultural practices. A comparison of present and anticipated land uses revealed existing gaps, which are mostly due to noncompliance with regulatory requirements. Only 73% of land meets the zoning established by Law No. 21, which provides the legal framework for the development and implementation of the PIOTA. Out of this area, 7% of these incompatible uses are located in fragile ecosystems of high ecological value (IDB, 2022).

Urban and demographic factors such as inadequate urban planning, population growth and urban sprawl have led to increased strains on the infrastructure to provide potable water, especially for indigenous communities who live on the PCW (Ministry of Foreign Affairs, 2022). At the same time, population growth has also led to the contamination of the region's land and rivers, due to reasons such as inadequate garbage and sewage systems and pollution by businesses (Ministry of Foreign Affairs, 2022). Out of the entire basin area, 2.4% is occupied by informal settlements and dispersed populated areas, with 0.8% situated within protected areas. The growth of human settlements in locations with steep slopes or in close proximity to rivers and/or streams poses a risk when combined with their social vulnerability, particularly when considering that 7.7% of the basin's population is classified as extremely vulnerable to flooding or landslides (IDB, 2022). Land rights are a major concern for these communities, especially with the potential impact of the Indio River project, which could affect around 2500 people (Vallecillos, 2024).

Farmers and ranchers, using roughly 23% of the watershed's land, are particularly affected by droughts as they are highly dependent on rainfall (IDB, 2022). The ACP (2023; 2020) is actively engaged in projects aimed at enhancing agricultural productivity and combating inefficient use of water for irrigation for the numerous small-scale farmers and coffee producers residing within the basin. For example, some residents receive financial incentives and technical support from the ACP to aid in the preservation of rainforests and sustainable land management practices (Moloney, 2024).

To address these anomalies, land-use categories consistent with the regional plan were incorporated in this new plan. An enhanced zoning criteria was also determined, outlining each zone with its links to regulatory aspects, including adherence to national and local regulations, preservation of natural and cultural assets, integration of resilience considerations, land use regulation, identification of new expansion areas, and regularisation of existing land uses within the territory, such as formalizing and legalizing informal settlements (IDB, 2022).

Yet some governance challenges for integrated land-use planning and disaster risk management lie ahead. At the national level, the PCW lacks dedicated planning tools for managing disaster risks, whether specific or integrated. However, at the regional level, planning instruments for disaster risk management do exist, yet they fail to incorporate considerations for climate change scenarios. Finally, the local level is equipped with planning instruments that actively account for climate change scenarios (IDB, 2022).

The formulation of the PIOTA involved a participatory process that encompassed 40 public participation activities. These sessions engaged over 860 institutional actors representing various sectors, including the productive sector, Consultative Councils, Local Committees, Municipalities, NGOs, and universities. As the PIOTA transitions into its implementation phase, new commitments will be essential to drive forward its objectives and realise its vision effectively (Madrid, 2022).

Recognising the essential necessity of preserving its rainforests and securing climate funding, Panama has launched a proactive conservation and restoration strategy. The country is actively phasing out deforestation and making steps to restore forest cover. By 2030, Panama aims to combat desertification and restore degraded land and soil, including areas impacted by desertification, drought, and floods (Ministry of Environment, n.d.).

7.3 Differential vulnerability

Although Panama presents an important logistics and financial area in the region, with progress led by trade services and facilitated by the Canal, the country continues to be ranked as one of the most unequal nations globally as per OECD's metric on income and the Gini Index on distribution of family income (OECD, 2017; CIA, 2021; IFRC, 2023; World Bank, 2024). Panama has a poverty rate of more than 20%, with Indigenous peoples and Afro-Panamians facing disproportionately higher rates of poverty (IFRC, 2023; World Bank, 2024). Moreover, there is sparse access to basic services, including a labor market with rural workers and individuals with low-level education lacking access to decent jobs. Almost half of all labor market participants lack access to social protection programs such as unemployment benefit programs (World Bank, 2023). In the Gatun Lake region, consisting of the Colón and La Chorrera districts, the percentage of people living in poverty ranges from below 10% to 30% in the townships of Ciricito and Arosemena in the Colón district and reaches 60% in the townships of Arosemena, Amador, and Obaldía in the La Chorrera district (IDB, 2022). Multi-dimensional poverty across these townships is driven primarily by inadequate education, precarity in work, and lack of access to water including potable water and solid waste management services (ibid).

Households living in poverty bear a larger burden of extreme weather and climate impacts (World Bank, 2023). In 2019, the multi-purpose survey (Encuesta de Propositos Múltiples) found that 19% of the poor are impacted by extreme climate and extreme weather events, compared to 8% reported by the middle class (ibid). Periods of low rainfall in Panama can lead to crop loss and drive poverty, especially for rural households that depend on subsistence farming (Borgen Project, 2017). This is especially true in Colón and La Chorrera where agriculture and livestock farming is the primary sector (IDB, 2022).

In addition to supplying water to the Panama Canal, Gatun Lake also provides drinking water to approximately 2.25 million people, more than half of the country's population (Moloney, 2024). During the present period of rainfall deficit, competing pressures of shipping and providing potable water have been a continued, contentious issue, with reports of lacking communication between forest villages and canal authorities (ibid.; Rodriguez, 2023). This contributed to existing public frustration towards the government regarding environmental issues and community rights (Moloney, 2024.; Millard & McDonald, 2024). Pre-existing public frustration and protests around environmental issues and social policy can compound frustrations driven by low rainfall. Protestors in March 2024 cited a lack of national policies for poverty reduction, unemployment rates, corruption, and a rise in insecurity linked to the drug trade in the country (Harkins, 2024; Moreno, 2024).

Much of the information available online about the low rainfall has centered on the Panama Canal as a place for trade and shipping logistics, with little coverage of its impact of droughts on surrounding communities and people dependent on Lake Gatun and its catchment.

7.4 Global shipping

The Panama Canal, a vital artery of global trade, is currently facing severe challenges due to historically low water levels, leading to disruptions that cascade across international shipping networks. Simultaneously, impacts are compounded by disruptions to the Suez canal, at a time when global shipping volumes and the size of shipping fleets continue to grow. This section examines the vulnerabilities and profound impacts these disruptions have inflicted on global shipping, economic dynamics, and local communities.

The canal's historical low water levels have necessitated transit restrictions, reducing the number of transits from the normal 38 to 24 per day since November 2023 (Wrabel, 2024), resulting in long queues at nearby ports as ships await their turn, potentially leading to up to 4,000 fewer ships passing through in 2024 (Ruiz & Shintani, 2024). Given the Panama Canal's pivotal role in global seaborne trade, handling approximately 5% of such trade and 40% of U.S. container traffic, the disruptions have sent shockwaves throughout international shipping networks (Dahl, 2024; Fleming, 2023; AP News, 2024). Unreliable passage through the canal has prompted some ships to seek alternative routes, further complicating supply chain logistics (Ruiz & Shintani, 2024; Millard, 2023).

These disruptions have not only economic ramifications but also social consequences, particularly for Panamanian communities reliant on the canal's economic activity. Reduced revenue for the Canal authority may lead to budget cuts, affecting local infrastructure and services (The Maritime Executive, 2023; Encinas, 2023). The livelihoods of Panamanians employed in canal-related industries, including port operations, logistics, and tourism, are also jeopardized. Job losses and income reductions in these sectors could have far-reaching implications for local families and communities, exacerbating socio-economic disparities. Additionally, the Canal is a significant source of revenue for the Panamanian government, providing around 6% of its GDP (Pianese, 2023). Its reduced operations may also jeopardize government finances and public services that support livelihoods (Ruiz & Shintani, 2024).

The impacts extend far beyond Panama, affecting global supply chains and economic stability. With the canal handling 5% of global shipping, disruptions have led to delayed shipments, increased fuel usage, and GDP losses (Ruiz & Shintani, 2024). Particularly affected are U.S. agricultural exports, valued at nearly $200 billion annually, with commodities like soybeans and corn heavily reliant on the canal for transit (Bamberg, 2024). Further, 22 and 26% of Chile and Peru's foreign trade pass through the canal, respectively, causing considerable economic impacts for these countries (Zumbish, 2024). The economic fallout from reduced canal capacity is estimated to range from $500 million to $700 million in 2024 alone (Los Angeles Times, 2024), exacerbating inflationary pressures worldwide (AP News, 2024). Research suggests that a 20% increase in shipping costs can boost the inflation rate by 0.15 percentage point a year later (Carriére-Swallow et al., 2023). Higher inflation can push more people into poverty, especially in developing countries where food security is threatened (Curtis et al., 2023; Dahl, 2024).

Finally, compounding these challenges are political events in the Red Sea, with attacks on ships significantly disrupting traffic through the Suez Canal (Ruiz & Shintani, 2024; UNCTAD, 2024). The concurrent disruptions in the Panama and Suez canals have forced more ships to take longer routes, exacerbating congestion and delays at US West Coast ports, driving up demand for trucking and rail services, and increasing GHG emissions (SOBEL, 2023). The impacts on freight rates, coupled with heightened inflationary pressures, underscore the urgent need for coordinated responses to safeguard global shipping and mitigate the socio-economic consequences of canal disruptions.

V&E conclusions

Panama is both a highly water-rich and water-dependent country, with the Panama Canal and the people around it all depending on this natural resource for continued prosperity. Rich in biodiversity, the country maintains a delicate balance between protecting its natural resources and people, and preserving the functioning of the water-intensive shipping corridor.

Urban expansion and unsustainable agriculture exacerbate land degradation in the Panama Canal Watershed, and the increased population strains natural resources, especially drinking water, heightening the impact of low rainfall in the region. While initiatives exist to increase the efficiency of water usage through the ACP's work with farmers on combating inefficient irrigation use, for example, there is an opportunity to do more to increase efficiency, especially as roughly 42% of the potable water produced is lost in the water distribution system. Over the past 20 years, efforts to protect forest cover have successfully decreased the net rate of deforestation, a positive advancement that can be further accelerated.

Indigenous and Afro-Panamanian communities face heightened vulnerability to drought impacts due to limited access to basic services, exacerbating poverty and water insecurity. Rural households in agricultural districts also suffer intensified poverty as crop loss worsens already precarious livelihoods, highlighting the interplay between climate vulnerability and economic deprivation. The transit restrictions linked to low water levels in the Panama Canal decrease ship traffic, causing disruptions in global shipping. Reduced revenue for the ACP could jeopardize employment and services in canal-related industries, and can, in turn, exacerbate socio-economic challenges. Economic impacts extend globally, affecting inflation rates and supply chains. Many ships now have to take longer shipping routes, exacerbating congestion and delays at other ports, and driving up demand for trucking and rail services, increasing costs and greenhouse gas emissions.

Competition for water resources between the Panama Canal and local communities exacerbates pre-existing tensions around inadequate poverty alleviation, corruption, and environmental rights. Balancing water for the Panama Canal amid urban expansion is critical to its continued success as a vital shipping route, especially as demand from the Canal is set to double by 2050.

Acknowledgements

WWA would like to acknowledge the Meteorology and Hydrology Branch, Panama Canal Authority, Republic of Panama, for providing station data used in this study.

Data availability

All time series used in the analysis are available via the Climate Explorer.

References

All references are given as hyperlinks in the text.

Appendix

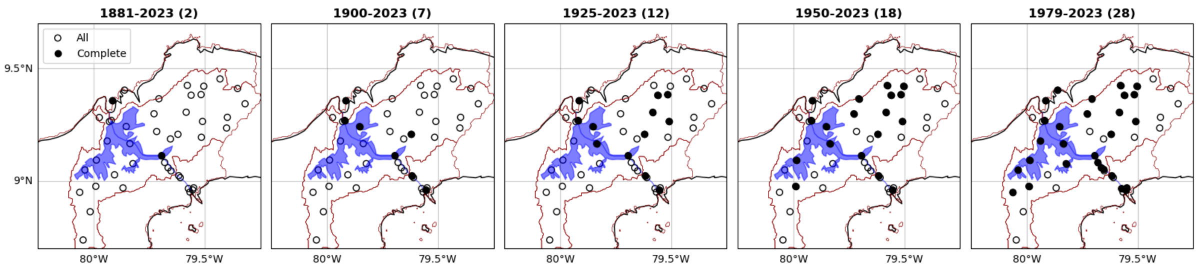

Figure A1: *Locations of subsets of stations with relatively complete stations over different periods, used in the sensitivity analysis in Section 3.2.1. Each map shows the locations of stations with data in more than 90% of years during each period as black dots. Numbers in brackets give the number of stations in each subset.*